1960

On inelastic buckling in steel, Proc. ASCE, 84 (EM2), p. 1581, (alos Trans. ASCE, Vol. 125, (1960), Reprint No. 124 (60-2)

G. Haaijer

B. Thurlimann

Welded Continuous Frames and Their Components

Progress Report No.22

Correction
p. 12 Eq (15)

ON INELASTIC BUCKLING IN STEEL

A Theoretical and Experimental Study With Recommendations for the Geometry of Wide-Flange Shapes in Plastic Design

by

Geerhard Haaijer and Bruno Thürlimann

This work has been carried out as a part of an investigation sponsored jointly by the Welding Research Council and the Department of the Navy with funds furnished by the following:

American Institute of Steel Construction
American Iron and Steel Institute
Institute of Research, Lehigh University
Column Research Council (Advisory)
Office of Naval Research (Contract No.39303)
Bureau of Ships
Bureau of Yards and Docks

Fritz Engineering Laboratory
Department of Civil Engineering
Lehigh University
Bethlehem, Pennsylvania

May, 1957

Fritz Laboratory Report No. 205E.9

TABLE OF CONTENTS

ABSTRACT

Plastic Design Methods assume that local buckling of flanges and webs of WF-Beams will not occur during the formation of plastic hinges. Such severe conditions made the re-examination of the problem of plate buckling in the inelastic range necessary.

In contradiction to accepted opinions it was found that steel columns and plates can be compressed beyond the yield point and even into the strain hardening range without buckling. Theoretical results for the required geometric proportions are presented and comparison is made to experimental results obtained from tests on model columns, angles and WF-beams.

Furthermore, consideration is given to the problem of buckling between the elastic limit and the yield stress.

2. INTRODUCTION

2.1 Statement of Problem

Present-day elastic design of steel structures is based on the concept of a specified safety factor against nominal yielding of the most stressed fibers. Concerning the detail design of flanges and webs of WF-beams and other plate elements, it is therefore sufficient that the yield stress can be reached without premature local buckling. However, newer methods of structural design, referred to as "Plastic Design", "Collapse Design", etc., propose to base the design on the actual load-carrying capacity of the structure. The working loads are determined as a specified percentage of the ultimate load. This ultimate load can only be realized if the members can undergo plastic deformations at a number of sections without local or lateral buckling, and a consequent fall-off in bending moment resistance. This process is generally referred to as the formation of plastic hinges and redistribution of moments. It is therefore evident that Plastic Design imposes more severe conditions on the local buckling characteristics of the plate elements of structural members and requires a reappraisal of the problem of inelastic buckling.

Extensive literature* exists on the buckling of columns and plates compressed beyond the elastic limit of the material. However, it is generally accepted that such elements made out of structural steel will invariably buckle once the yield stress is reached. The following statements from reference (1) may be quoted:

---

*For a summary, references (1) and (2) may be consulted.

On page 159:

> "To obtain a compressive load on a bar larger than the load producing the yield-point stress, it is necessary to prevent the bar from lateral buckling at the yield point by applying some lateral constraint."

And on page 385:

> "Experiments show that, when the compressive stress reaches the yield point of the material, ...the plate buckles for any value of the ratio b/h."

Essentially the same conclusions must be drawn from the equations for inelastic buckling presented in reference (2). Both the column and plate buckling equations -- equations (21) and (653) -- contain the factor $\tau=E_t/E$. When the yield stress is reached, the tangent modulus E_t reduces to zero and hence buckling seems to be unavoidable.

At first glance, therefore, it may appear impossible to compress structural steel elements beyond the initial yield strain, ε_f, (see Fig.1a) without buckling. This situation would invalidate one of the basic assumptions of plastic analysis and hence make it inapplicable to structural design.

Fortunately this reasoning is in error. Whereas theories, as presented in references (1) and (2), give a fair account of buckling in the elastic range and in the inelastic range between the proportional limit and the initial yield point strain, ε_f, they are not applicable to cases beyond this range. A study of the stability of plates stressed into the strain-hardening range has been presented in reference (3). This paper constitutes a continuation and extension including pertinent test data.

2.2 Inelastic Behavior of Structural Steel

For a proper understanding of the new approach presented in this paper a short discussion of the inelastic behavior of structural steel is necessary. Fig.1a shows the well-known stress-strain diagram of a coupon in tension or compression. In the elastic range the material exhibits homogeneous and isotropic behavior. Yielding commences rather abruptly without any significant indication of a proportion limit. At the yield stress, σ_o, considerable straining takes place without an increase in stress such that the tangent modulus, E_t, seems to reduce to zero. However, it should be kept in mind that the strain, ε, is an average strain, derived from the measurement of an elongation (or shortening) over a certain gage length. Actually there is no material within this gage length at a strain between ε_f and ε_o. The mechanism of yielding is discontinuous, taking place in small slip bands by a sudden jump of strain from ε_f to ε_o. The slip bands form successively, starting at a "weak" point (inclusion, point of stress concentraction, etc.) and then spread out into the rest of the specimen.*

Therefore, during yielding some of the material is still elastic while the yielded zones have reached the point of strain-hardening, ε_o. The material within the coupon is therefore heterogeneous. Once all material has been strain-hardened, the stress starts to increase again. Once again, all of the material has identical physical properties and hence is homogeneous. However, slip produced such changes that it is no longer isotropic --

*For an informative description see reference (4) p.297.

i.e., its properties are now direction dependent. If proper consideration is given to these physical facts the behavior of compression elements of structural steel in the yield and strain hardening range can be explained and predicted.

3. THEORETICAL INVESTIGATION

3.1 Inelastic Column Buckling

Before treating the problem of plate buckling, it may be advantageous to first summarize the behavior of columns. The elastic buckling stress of a slender column is given by:

$$\sigma_e = \frac{\pi^2 E}{(\ell/r)^2} \qquad \text{- - - - - - - - - - - - (1)}$$

where σ_e = elastic buckling stress

E = modulus of elasticity

ℓ = effective column length

r = radius of gyration

In the inelastic range the theoretical stress at which bifurcation of equilibrium will occur (bending commences) is characterized by the tangent modulus stress[2]

$$\sigma_t = \frac{\pi^2 E_t}{(\ell/r)^2} \qquad \text{- - - - - - - - - - - - (2)}$$

where

E_t= tangent modulus

The maximum stress lies between σ_t and the reduced modulus stress

$$\sigma_r = \frac{\pi^2 E_r}{(\ell/r)^2} \qquad \text{- - - - - - - - - - - - (3)}$$

For a rectangular section the reduced modulus is given by[1]

$$E_r = \frac{4 E E_t}{(\sqrt{E} + \sqrt{E_t})^2} \qquad \text{- - - - - - - - - - - - (4)}$$

For design purposes the possible increase of the maximum stress beyond the tangent modulus stress is generally neglected. If the tangent modulus E_t is given, the behavior of a column can be predicted.

On the basis of the simplified stress-strain diagram (Fig. 1b) buckling would be elastic up to the yield point stress, σ_o. The slenderness ratio (ℓ/r) corresponding to initiation of yielding is obtained by inserting into equation (1) the values $\sigma_e=\sigma_o$ and E. For smaller values of ℓ/r buckling will not occur immediately once the yield strain ϵ_f is reached but yielding will commence, with the formation of slip bands somewhere along the length of the specimen. For a pin-ended column the worst situation will occur if yielding starts to spread from the center. The bending stiffness of the middle part is greatly reduced to E_oI, E_o being the tangent modulus of the zone which has reached strain-hardening. The end-pieces are still elastic and hence their bending stiffness is given by EI (see Fig. 2, case a). Assuming that the column is continuously compressed such that buckling will occur without strain reversal, the buckling condition is given by the following transcendental equation:*

$$\sqrt{E_o/E}\,\tan\frac{\varphi\pi}{\sqrt{E_o/E}}\,\zeta\,\tan\varphi\pi\left(\frac{1}{2}-\zeta\right)=1 \qquad \cdots(5)$$

where

$\varphi^2 = \sigma_{cr}/\sigma_e$

σ_{cr}= buckling stress

σ_e = elastic buckling stress

ζ = parameter specifying extent of yielded zone as shown in Fig. 2, case a).

*See Ref. (1), p.128 (Some changes in notation have been made).

For given values of E_o/E and ζ, values of φ can be derived by trial and error. As buckling occurs within the plastic range--i.e. the critical stress σ_{cr}, is equal to the yield stress σ_o the slenderness ratio ℓ/r can be computed:

$$\sigma_{cr} = \sigma_o = \varphi^2 \sigma_e = \frac{\varphi^2 \pi^2 E}{(\ell/r)^2}$$

or:

$$(\ell/r)^2 = \varphi^2 \frac{\pi^2 E}{\sigma_o} \quad \text{- - - - - - - - - - - - (6)}$$

The shortening of the column, $\Delta\ell$, is given by:

$$\Delta\ell = \varepsilon_f (1 - 2\zeta)\ell + 2\varepsilon_o \zeta \ell$$

and the average strain at which buckling occurs:

$$\varepsilon_{cr} = \Delta\ell/\ell = (1 - 2\zeta)\varepsilon_f + 2\zeta\varepsilon_o \quad \text{---- (7)}$$

Numerical results for Equation (7) are shown in Fig. 2, curve (a), derived on the basis of the following material constants:

$E = 30{,}000$ ksi

$E_o = 800$ ksi

$\varepsilon_f = 1.1 \times 10^{-3}$

$\varepsilon_o = 14 \times 10^{-3}$

$\sigma_o = 33$ ksi

The yield stress, σ_o, is reached for a slenderness ratio $\ell/r = 94.9$, the corresponding strain being the yield strain ε_f. For smaller slenderness ratios, ℓ/r, the buckling stress σ_{cr} remains constant at the yield stress level. However, buckling will only occur after the yielded zone at the center has spread over a length $2\zeta\ell$ resulting in a great reduction of the bending stiffness over this section.

The average critical strain changes at first very little with decreasing ℓ/r, but increases rapidly for values of ℓ/r

smaller than 30. Finally, for $\ell/r=15.4$ the entire length is strain-hardened before buckling occurs. If ℓ/r is still further reduced the critical stress will increase above the yield stress σ_o. All material being strain-hardened, the tangent modulus E_t for the entire length is given by the slope of the stress-strain curve in the strain-hardening range.

Another extreme assumption would be that yielding spreads symmetrically from both ends. The corresponding curve (b) in Fig.2 is considerably above the previously derived curve (a).

The foregoing reasoning is substantiated by the results of 37 tests on small model columns which are also plotted in Fig.2.* The average yield stress of the steel used was about 35 ksi. Unfortunately no records of the strain-hardening strain ε_o and the strain-hardening modulus E_o are available. Almost all test points lie between the two theoretically derived curves. The actual yielding may occur anywhere between these two extreme assumptions.

The experimental indications however are that strains larger than the yield strain ε_f can be reached without buckling. For sufficiently small ℓ/r-values the point of strain-hardening, ε_o, can be reached and even exceeded. Corresponding test results will be given in a subsequent section.

If theoretical predictions, based on Equations (1) and (2) and a tangent modulus E_t derived from a coupon stress strain diagram, are compared to the actual behavior of structural steel columns such as WF-sections, built-up members, etc., a considerable

*The test results were obtained from Mr. P.C. Paris, instructor at Lehigh University. The tests were performed by him and Dr. T.A. Hunter at the University of Michigan under the direction of Prof. J.A. Van den Broek.

discrepancy is observed in the intermediate column range $30 \leq \ell/r \leq 110$, the theoretical predictions being always considerably too high. This situation generally has been attributed to initial imperfections, accidental end eccentricities, etc. Bleich introduced an "effective" coefficient, $\tau = E_t/E$ -- Eq. (64) reference (2) -- much below the actual τ based on a coupon stress strain curve, in order to preserve the applicability of Eq. (2) to inelastic buckling. However recent theoretical and experimental investigations cleared up the situation very conclusively by attributing this discrepancy to the presence of residual stresses[5][6]. The proportional limit of an axially loaded column is reached when the sum of the applied stress P/A and the maximum compressive residual stress reaches yielding. The subsequent behavior of the column depends on the distribution of the residual stresses and the direction of buckling -- i.e., weak or strong axis buckling. However for ℓ/r approaching about 15, the strain-hardening range is reached and the influence of residual stresses is completely wiped out. From there on the buckling load is governed by the tangent modulus, E_t, only.

3.2 Inelastic Plate Buckling Under Uniform Compression

In the previous section the possibility of a column buckling at stresses above the yield stress, σ_o, was shown. It can therefore be assumed that the same may hold true for plates. The objective of the following analysis is the derivation of a plate buckling equation which is applicable to the strain-hardening range. The behavior of plates which buckle in the intermediate range between the proportional limit (sum of applied and residual stress equal to yield stress) and the strain hardening range is governed

by the presence and distribution of residual stresses. No direct solution of this problem has yet been developed. However, a reasonable transition curve will be proposed.

During yielding the material changes its physical properties such that at strain-hardening the initially isotropic material has become orthotropic -- i.e., the properties are direction dependent. In case of plane stress the stress and strain relations of such a material can be expressed in the following general form:

$$d\varepsilon_x = \frac{1}{E_x} d\sigma_x - \frac{\nu_y}{E_y} d\sigma_y$$

$$d\varepsilon_y = -\frac{\nu_x}{E_x} d\sigma_x + \frac{1}{E_y} d\sigma_y \qquad ---(8)$$

$$d\gamma_{xy} = \frac{1}{G_t} d\tau_{xy}$$

where

ε = normal strain

γ = shear strain

σ = normal stress

τ = shear stress

E_x = tangent modulus in x direction

E_y = tangent modulus in y direction

G_t = tangent shear modulus

ν_x = coefficient of dilatation for increase in σ_x

ν_y = coefficient of dilatation for increase in σ_y

If Equations(8) are valid for the entire plate cross-section, the expressions for the bending and twisting moments in terms of the transverse plate deflection w, become

$$M_x = -D_x I \left(\frac{\partial^2 w}{\partial x^2} + \nu_y \frac{\partial^2 w}{\partial y^2} \right)$$
$$M_y = -D_y I \left(\frac{\partial^2 w}{\partial y^2} + \nu_x \frac{\partial^2 w}{\partial x^2} \right) \qquad \text{- - - - - - - - - (9)}$$
$$M_{xy} = -2G_t \frac{\partial^2 w}{\partial x \partial y}$$

where

$I = \frac{t^3}{12}$

t = thickness of plate

$D_x = \frac{E_x}{1-\nu_x \nu_y}$

$D_y = \frac{E_y}{1-\nu_x \nu_y}$

The above expressions imply that buckling occurs without strain reversal. From these relations the following general expressions for the buckling strength of uniformly compressed, rectangular plates can be derived as shown in Reference (3):

(1) Loaded edges x=0 and x= ℓ hinged, unloaded edge y=0 hinged and unloaded edge y=b free. (see Fig.3)

$$\sigma_{cr} = \left(\frac{t}{b}\right)^2 \left[\frac{\pi^2}{12} D_x \left(\frac{b}{\ell}\right)^2 + G_t \right] \qquad \text{---(10)}$$

where

t = thickness of plate

b = width of plate

ℓ = length of plate or half-wave length

For a long plate the first term can be neglected and the buckling stress becomes:

$$\sigma_{cr} = \left(\frac{t}{b}\right)^2 G_t \qquad \text{- - - - - - - - - (11)}$$

(2) Same as case 1, but unloaded edge y=0 fixed.

The minimum value of the buckling stress occurs when the length-to-width ratio is

$$\frac{\ell}{b} = 1.46 \sqrt[4]{\frac{D_x}{D_y}} \qquad \text{- - - - - - - - - - (12)}$$

Then

$$\sigma_{cr} = \left(\frac{t}{b}\right)^2 \left[0.769 \sqrt{D_x D_y} - 0.270 (D_{xy} + D_{yx}) + 1.712 G_t\right] \text{-(13)}$$

$$D_{xy} = \nu_y D_x \qquad D_{yx} = \nu_x D_y$$

(3) Loaded edges x=0 and x=ℓ hinged, unloaded edges y=$\pm$ d/2 hinged. (See Fig.4)

The minimum value of the buckling stress is obtained for the following value of the length-to-width ratio:

$$\frac{\ell}{d} = \sqrt[4]{\frac{D_x}{D_y}} \qquad \text{- - - - - - - - - (14)}$$

Then

$$\sigma_{cr} = \frac{\pi^2}{12} \left(\frac{t}{d}\right)^2 \left[2 \sqrt{D_x D_y} + D_{xy} + D_{yx} + 4 G_t\right] \text{--- (15)}$$

(4) Same as case 3, but unloaded edges y=$\pm$ d/2 fixed.

The minimum value of the buckling stress is obtained for

$$\frac{\ell}{d} = 0.66 \sqrt[4]{\frac{D_x}{D_y}} \qquad \text{- - - - - - - - - (16)}$$

Then

$$\sigma_{cr} = \frac{\pi^2}{12} \left(\frac{t}{d}\right)^2 \left[4.554 \sqrt{D_x D_y} + 1.237 (D_{xy} + D_{yx}) + 4.943 G_t\right] \qquad \text{----- (17)}$$

Several theories of plasticity are available for the determination of the moduli E_x, E_y, ν_x, ν_y and G_t. The various theoretical predictions as applied to the plate buckling problem are summarized in Table 1. Obviously, there are significant discrepancies between these theories. From the point of view of the mathematical theory of plasticity the stress-strain relations should be of the incremental type; only the stress-strain law used by Handelman and Prager[11] satisfies this condition. All theories except the last one can, therefore, be discarded.

Although the stress-strain law of Reference (11), with the second invariant of the deviatoric stress tensor as the loading function, has been verified experimentally by combined compression and torsion tests on tubes of mild steel stressed into the strain-hardening range[12], it cannot be applied without modification to the plate buckling problem. In Reference (3) it is shown how effective values of the moduli can be obtained from an incremental stress-strain relationship. From the stress-strain curve for the strain-hardening range of mild steel

$$\varepsilon - \varepsilon_0 = \frac{\sigma - \sigma_0}{E_0} + k\left(\frac{\sigma - \sigma_0}{E_0}\right)^m$$

Ramberg Osgood eq.

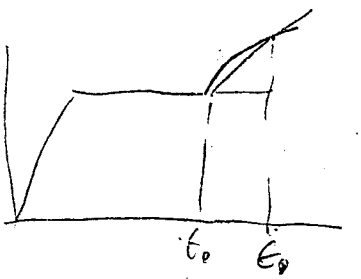

with

E_0 = 900 ksi

k = 21

m = 2

the following values of the moduli were found to be applicable:[3]

D_x = 3,000 ksi

D_y = 32,800 ksi

$D_{xy} = \nu_y D_x = \nu_x D_y$ = 8,100 ksi

G_t = 2,400 ksi

The above developed expressions for the buckling strength of orthotropic plates can only be applied if all material is strained into the strain-hardening range ($\varepsilon \geq \varepsilon_0$). In the intermediate range transition curves can be developed as in the case of column buckling (see Fig. 2).

Consider for instance a flange of length 2ℓ. The loaded edges $x=0$ and $x=2\ell$ are fixed, the unloaded edge $y=0$ is hinged and the unloaded edge $y=b$ is free.* For the simplified stress-strain

*This example has been chosen as a basis of comparison of the theory with the results of tests on plates with these boundary conditions presented in Chapter 4.

curve of Fig. 1b the elastic solution is valid for $\sigma_{cr} < \sigma_o$ and obtained from Equation (10) by substituting the elastic values of the moduli. Thus

$$\sigma_{cr} = \left(\frac{t}{b}\right)^2 \left[\frac{\pi^2 E}{12(1-\nu^2)}\left(\frac{b}{\ell}\right)^2 + G\right] \quad \text{---------- (19)}$$

If the geometry of the specimen (given by b/t, b/ℓ) is such that σ_{cr} from equation (19) would exceed the yield stress, σ_o, yielding will occur before the plate buckles, the stress remaining at the yield value σ_o. In order to find a solution for this case it is necessary to assume a certain distribution of the strain-hardened zones, for example, yielding starts at the ends and spreads towards the middle. This assumption seems to be reasonable in view of the fixed-end restraints and has also been observed during tests.

The middle section, being still elastic, is practically rigid compared with the yielded zones of length $\zeta\ell$. Assuming that only the latter will deform gives

$$\sigma_{cr} = \sigma_o = \left(\frac{t}{b}\right)^2 \left[\frac{\pi^2 D_x}{12}\left(\frac{b}{\zeta\ell}\right)^2 + G_t\right] \quad \text{---------- (20)}$$

The corresponding average critical strain is

$$\varepsilon_{cr} = (1-\zeta)\varepsilon_f + \zeta\varepsilon_o \quad \text{---------- (21)}$$

Equations (20) and (21) are applicable to plate elements that are free of residual stresses (for example, annealed specimens). However, as delivered specimens contain in general residual stresses of considerable magnitude such that partial yielding will set in at an applied stress considerably below the yield stress. In the following a more realistic approach to the range $\sigma_p < \sigma_{cr} < \sigma_o$ will be discussed. The elastic solution is only valid up to a limiting stress σ_p. The magnitude of σ_p is determined such that the sum of

the applied stress σ_p and the maximum residual compressive stress σ_R equals the yield stress σ_o. Hence the stress σ_p corresponds to the "effective proportional limit" of the specimen.

3.3 Buckling at Stresses Below the Yield Stress

The elastic buckling stress, σ_e, of a perfectly plane plate of isotropic material, subjected to forces acting in its plane, is given by:

$$\sigma_e = k \frac{\pi^2 E}{12(1-\nu^2)} \left(\frac{t}{b}\right)^2 \qquad (22)$$

where

k = plate buckling coefficient

This equation and the expression for the elastic buckling stress of a column, Equation (1), can be written in dimensionless form as follows:

$$\frac{\sigma_e}{\sigma_o} = \frac{1}{\alpha^2} \qquad (23)$$

where for a column

$$\alpha = \frac{\ell}{\pi r}\sqrt{\frac{\sigma_o}{E}} \qquad (24)$$

and for a plate

$$\alpha = \frac{b}{\pi t}\sqrt{\frac{12\sigma_o(1-\nu^2)}{k E}} \qquad (25)$$

Equation (23) is valid for values of α larger than a certain limiting value α_p (See Fig.5). The corresponding limiting stress is σ_p. As indicated before the sum of this limiting stress and the maximum residual stress equals the yield stress σ_o. From this point, $(\sigma_p/\sigma_o, \alpha_p)$, a transition curve must be followed to the point where the buckling stress equals the yield stress, $(\sigma_{cr}/\sigma_o = 1, \alpha_o)$. If a specimen reaches this point all its material has been yielded

and reached the strain-hardening range. The transition curve can generally be taken in the following form

$$\sigma_{cr}/\sigma_o = 1 - \left(1 - \frac{\sigma_p}{\sigma_o}\right)\left(\frac{\alpha - \alpha_o}{\alpha_L - \alpha_o}\right)^n \quad \text{--- --- (26)}$$

For a column the value of α_o is relatively small and the influence of strain-hardening is, therefore, generally neglected by taking $\alpha_o=0$. It has been shown by Huber[5], that the shape of the transition curve for WF columns depends on the distribution of the residual stresses and the axis about which the column buckles (weak or strong axis). The magnitude of the residuals determines the value of σ_p/σ_o . Actual measurements of residual stresses in WF shapes have furnished rather high values. In order to be conservative, σ_p/σ_o for most WF shapes should be taken equal to 0.5.

For WF Columns the influence of residual stresses is most pronounced if buckling takes place about the weak axis. The transition curve was found to be approximately a straight line ($n=1$, $\alpha_o=0$). When the column fails by bending about the strong axis a quadratic parabola, ($n=2$,$\alpha_o=0$) is a good approximation of the transition curve.

For plate buckling the influence of residual stresses will be less severe. Indeed, the buckling stress is not only dependent on the modulus E_x in the direction of the compressive loads, but also on the modulus E_y in the transverse direction and the shearing modulus G_t. However, yielding affects the latter to a much lesser degree than E_x (see equations 8, 10 to 17 and 18). This influence can be taken into account through a higher value of n. However, the transition curve given by Equation (26) can at the

most be tangent to the elastic solution given by Equation (23). From this condition the limiting value of n is found:

$$n_{max} = \frac{2(\alpha_L - \alpha_o)}{\alpha_L(\alpha_L^2 - 1)} \quad - - - - - - - (27)$$

It is suggested that this value be used for all cases of plate buckling.

Finally, the problem remains to determine the values of α_p and α_o. Equation (23) gives the value of α_p by substituting $\sigma_e = \sigma_p$, where σ_p is the effective proportional limit. For structural wide-flange shapes it is conservative to take $\sigma_p/\sigma_o = 0.5$. Thus $\alpha_p = \sqrt{2}$. Furthermore, the following values of α_o are determined from Equations (2), (11), (13), (15) and (17) respectively by substituting the given values of the moduli. In parenthesis the corresponding values of ℓ/r, b/t or d/t are given for $\sigma_o = 36$ ksi.

Columns	: $\alpha_o = 0.173$ ($\ell/r = 15.7$)
✓ Long hinged flanges	: $\alpha_o = 0.455$ (b/t=8.15)
Fixed flanges	: $\alpha_o = 0.461$ (b/t=14.3)
Hinged webs	: $\alpha_o = 0.588$ (d/t=32.3)
Fixed webs	: $\alpha_o = 0.579$ (d/t=42.0)

The above table suggests that the values of α_o depend only on the type of compression element (column, flange or web plate) and are nearly independent of the amount of restraint. The problem can, therefore, be somewhat simplified by taking for columns $\alpha_o = 0.17$, for flanges (plates with one free edge) $\alpha_o = 0.46$, and for webs (plates supported along all four edges) $\alpha_o = 0.58$. These values are used subsequently in Fig. 23 where comparison to test results is made.

The strain $\varepsilon_{cr.}$ at which buckling of the web plate occurs and the corresp. depth to thickness ratio d/t is of importance.

3.4 Inelastic Plate Buckling under Combined ~~Buckling~~ Bending and Compression

An extension of the previous considerations to cases of plates subjected to bending and axial load is of practical importance. The web of a WF-beam subjected to a bending moment M and axial load P presents such a case. Depending on the ratio of P/P_y, P_y being the yield load of the axially loaded member and equal to $\sigma_o A$, the neutral axis may lie inside or outside of the web.

First of all, the plate buckling coefficient k must be determined. The minimum values of k for a stress distribution of a fully plastified section are shown in Fig.6. In this figure, d corresponds to the depth of the web and y_o fixes the position of the neutral axis. The values were determined by equating the work of the external forces to the dissipation of the internal energy at the moment of buckling, using the moduli given in Chapter 3.2.

Secondly, the strain ε_{cr} at which buckling of the web plate occurs and the corresponding depth to thickness ratio d/t is of importance. For an expedient solution of this rather involved problem recourse to subsequently described test results is made. Fig.7 shows experimentally determined values of α as a function of the critical strain ε_{cr} for uniformly compressed webs. The parameter α is defined by equation (25) - with depth d instead of width b -:

$$\alpha = \frac{d}{\pi t}\sqrt{\frac{12\,\sigma_o(1-\nu^2)}{kE}} \qquad \text{- - - - - - - - (28)}$$

and is hence proportional to the d/t ratio. Turning now to the problem at hand, the maximum strain of the compression flange is taken as ε_m. As the strain varies linearly over the depth of

the section the mean strain of the compression zone in the web is $\varepsilon_m/2$. Using this latter value in entering Fig.7 the following values of α are found:

For: $\varepsilon_m/\varepsilon_f = 12$: $\alpha = 0.58$

$\varepsilon_m/\varepsilon_f = 8$: $\alpha = 0.60$

$\varepsilon_m/\varepsilon_f = 4$: $\alpha = 0.69$

The resulting curves for the critical d/t ratios are plotted in Fig.8 for the specific values indicated.

Values of d/t corresponding to σ_o different from $\sigma_o = 33$ ksi are obtained by multiplying d/t by $\sqrt{33 \text{ ksi}/\sigma_o}$.

4. EXPERIMENTAL INVESTIGATION

4.1 Compression Tests on Short Rectangular-Columns

Contrary to commonly accepted opinion, it was stated above that buckling of columns at stresses above the yield stress should be possible without special precautions to prevent buckling at the yield stress. In order to verify this statement experimentally, a number of compression tests on short model columns of rectangular cross-section were carried out. The dimensions of the specimens, cut from the flange of an 8WF40 section, (ASTM A-7 steel) were chosen such that buckling in the strain-hardening range could be expected (see Table 2). The test set up is shown in Fig.9. The columns were placed flat-ended in a hydraulic testing machine. During the tests simultaneous load, strain and lateral deflection readings were taken.

The maximum loads divided by the area are plotted in Fig. 11, and compared with the tangent-modulus and reduced modulus loads.

Confirmation is obtained of the prediction that the maximum load lies between the tangent and reduced-modulus load . The behavior of the columns is illustrated in Fig.12 showing the lateral deflection of the column as a function of the strain. It is obvious from these curves that the columns can reach the strain-hardening range without deflecting excessively. The critical strains corresponding to the tangent-modulus loads are indicated by arrows. Indeed, at these points the deflections start to increase at an accelerated rate, confirming once again that the tangent modulus load is the load at which bending commences.

4.2 Compression Tests on Angles

The next phase in the experimental program was the verification of the inelastic plate buckling theory. For this purpose a number of compression tests on angles were carried out. When buckling torsionally, the flanges of an equilateral angle act as two plates, hinged along the heel and free along the outstanding edge. The loaded ends of the angle columns were fixed in the testing machine against rotation. Fig.10 shows one of the specimens after testing. The dimensions of all specimens are given in Table 3. The specimens were machined from a 6x6x3/8 (14.9 lb) angle, ASTM A-7 steel, by reducing the width of the leg to the desired dimension b. Table 3 indicates that six specimens were tested after complete annealing and two specimens were in the "as-delivered" state. Material properties as obtained from coupon tests are summarized in Table 4.

Fig.13 shows the obtained stress vs. average axial strain curves. Furthermore, the rotations of the center section were

The critical strain is defined as the strain at which the rotation starts to increase more rapidly.

measured. They are plotted as a function of the average strain in Fig.14. In both figures the experimentally determined critical strains are indicated by arrows. The critical strain is defined as the strain at which the rotation starts to increase more rapidly than it did initially. Specimens A41 and A42 did not buckle torsionally but failed by bending about the weak axis. Buckling occurred in the strain-hardening range, thus proving once more that buckling does not necessarily take place at the yield stress. The results of all tests on angles are summarized in Table 5.

The theoretical solution for the strain-hardening range is given by Equation (10) and for the yielding range by Eqaution (20) and Equation (21). Fig.15a shows a plot of ζ (parameter defining extent of yielded zones) vs. b/t as obtained from Equation (20). As elastic deformations have been neglected in the derivation of this equation b/t= ∞ for ζ =0 (rigid-plastic solution). From equation (19), however, it follows that for ζ =0, b/t=20.7. Knowing the rigid-plastic solution and the point for ζ =0, corresponding to the limit of the elastic solutions, the elastic-plastic solution is sketched as a dotted line in Fig.15a. The critical strain can then be determined from Equation (21).

The obtained ε_{cr} vs. b/t curves are compared with test results in Fig.15b. The theoretical curve describes adequately the behavior of the test specimens.

4.3 Compression and Bending Tests on Wide-Flange Shapes

Six wide-flange shapes were tested under two loading conditions:

(a) Axial compression (Tests D1,D2,D3,D4,D5,D6)

(b) Pure bending (Tests B1,B2,B3,B4,B5,B6)

critical strain: is defined as the average strain at which the deflection starts to increase more rapidly

The dimensions of all specimens are given in Table 6. Material properties obtained from coupon tests are summarized in Table 7. The compression specimens were placed flat-ended in a testing machine, the length being divided in three gage lengths over which the change in length was measured directly with 0.0001" Ames dials. The set-up of the compression tests is shown in Fig.21a. The bending specimens were loaded symmetrically by two concentrated loads (see Fig.21b) and the dimensions were chosen such that shear failure was avoided. Again changes in length of the flanges were measured.

The resulting P/A vs. ε_{av} curves for the compressions tests and M/Z vs. ε_{av} curves for the bending tests are plotted in Figs. 16 and 17 respectively, where

P = compressive load

A = area of cross-section

M = moment

Z = plastic section modulus

ε_{av} = average strain at center of compressed flange.

Furthermore, with the aid of a dial gage lateral deflection measurements were taken along the edges of the flanges and the center of the webs (see Fig. 18). For the bending tests the lateral rotation was measured at mid-span of the beam. The loading points were supported against lateral rotation. The observations of web deflection, flange buckling and lateral rotation from test B3 are plotted in Fig.18 as a typical example. From these curves the critical strains are obtained as indicated by arrows in Figs. 16 and 17. As mentioned above, the critical strain is defined as

the average strain at which the deflection starts to increase more rapidly than it did initially. The results of all tests are summarized in Table 8.

The results of those tests where flange buckling was predominant are shown in Fig.19. The results of tests D4 and D6 are omitted because web buckling occurred first and caused premature flange buckling. Specimen B4 did not develop a major flange buckle but failed by lateral-torsional buckling. This result is therefore eliminated from Fig.19. The critical strains are plotted as a function of b/t and are compared with theoretical solutions* for different values of the coefficient of restraint, β . This coefficient represents the restraints provided by the web to the flange. In case of elastic restraint, where ψ = moment per unit length required for a unit rotation, the coefficient of restraint becomes

$$\beta = \frac{\psi b}{2 D_y I} \qquad \text{- - - - - - - - - - - - (29)}$$

From the tests results it is seen that β has a value of the order of 0.01.

For the cases where web buckling occurred first (Tests D4 and D6) or simultaneous with flange buckling (Test D2) the results are plotted in Fig.20 and are compared with the theoretical solution given by Equations (15) and (17).

It is concluded that the theoretical curves give a good description of the actual behavior of flanges and webs.

Some typical examples of wide-flange specimens after testing are shown in Fig.22. Specimen D6 failed by web buckling after

---

*The theoretical curves are taken from Reference 3.

just reaching the yield point stress. The yielded material is concentrated at the top of the specimen. Simultaneous web and flange buckling caused specimen D2 to fail after just being completely strain-hardened while specimen D5 failed by flange buckling in the strain-hardening range. Of the bending specimens B2 and B6 failed because of flange buckling but B4 buckled laterally without developing a flange buckle.

4.4 Summary of Test Results

All test results are summarized in Fig.23 showing σ_{cr}/σ_o as a function of the dimensionless parameter α. The figure clearly illustrates the difference in the behavior of columns, flanges and webs. The values of α for which the strain-hardening range can be reached are confirmed by the test results and can be taken as follows:

Column Buckling	$\alpha_o = 0.17$
Flange Buckling	$\alpha_o = 0.46$
Web Buckling	$\alpha_o = 0.58$

For flanges and webs, the shape of the transition curves (the plotted curves correspond to the maximum value of the exponent n, Equation (27)) should be considered as reasonable interpolations in the absence of sufficient test results in this particular region. Concerning the transition curve for the columns considerable experimental and theoretical data are available.[5]

5. RECOMMENDATIONS FOR THE GEOMETRY OF WIDE-FLANGE SHAPES IN PLASTIC DESIGN

5.1 Flanges

The following recommendations are directly based on the above presented theoretical and experimental investigation. Flanges of WF shapes can be strained into the strain-hardening range if $\alpha \leq 0.46$. In general this is a sufficient requirement for the development of plastic hinges. Furthermore, buckling is then not accompanied by a sudden drop of the load (see results of tests A31-32-33, D2 and B2 in Figs.13, 16 and 17 respectively). Consequently the following recommendation can be given:

> The ratio of the outstanding width to the thickness of flanges, b/t, shall not exceed the following values depending on the value of the yield stress, σ_o:
>
> for σ_o = 33 ksi : $b/t \leq 8.7$, and
>
> for σ_o = 36 ksi : $b/t \leq 8.3$.

5.2 Webs

(a) Uniformly Compressed Webs:

The results of compression tests on WF shapes failing by web buckling showed that for α=0.77 (Test D6) the yield stress can just be reached and for α=0.57 (Test D2) the section can be uniformly compressed up to the strain-hardening range. For a section subjected to an axial load only, the first attainment of the yield stress is generally a sufficient requirement. In this case, therefore, the following recommendation can be given:

If a section is subjected to an axial load only, the ratio of the distance between the center planes of the flanges over the thickness of the web, d/t, shall not exceed the following values depending on the magnitude of the yield stress σ_o:

for $\sigma_o = 33$: $d/t \leq 44$, and

for $\sigma_o = 36$: $d/t \leq 42$.

(b) Webs in Compression and Bending:

WF-Members subjected to axial load P and bending moment M may be required to deform plastically. Obviously the critical depth/thickness ratio, d/t, depends not only on the stress distribution but also on the required maximum strain ε_m of the compression flange. Curves relating the critical d/t to the stress distribution (parameter $P/\sigma_o A_w$) and a given maximum strain (parameter $\varepsilon_m/\varepsilon_f$) were derived in Chapter 3.4 and are shown in Fig.8. Based on these results the following recommendation is made:

If a WF section is subjected to axial load and bending moment the d/t ratio shall not exceed the values given in Fig.8. Except in cases requiring large rotations the curve for $\varepsilon_m/\varepsilon_f=4$ can be used.

Values of d/t for a yield stress σ_o different from 33 ksi may be obtained by multiplying the ratio by $\sqrt{33 \text{ ksi}/\sigma_o}$. From the curves of Fig.8 three specific examples of P/P_o vs. allowable d/t ratios were investigated and are shown in Fig.24. It can be seen that the 12JR11.8 section, for example, is not recommended for use in plastic design, the 12B14 section can be used if $P/P_o \leq 0.08$ and the 36WF108 if $P/P_o \leq 0.135$.

6. SUMMARY

Contrarily to commonly accepted opinions columns and plates of structural steel can be compressed beyond the yield stress level and even into the strain-hardening range, provided certain geometric conditions are met. After shortly discussing the discontinuous yielding process of structural steel the values of these geometric conditions as slenderness ratio ℓ/r for columns and width-thickness ratio for plates are derived theoretically. The interesting observation is made that plates are reaching the strain-hardening range with a relatively smaller reduction in the d/t-ratio than the corresponding reduction in ℓ/r for columns.

The findings are substantiated by a series of tests on rectangular bars in axial compression, on angles and WF sections in compression and WF members in bending.

The results are used to specify the geometric cross-section proportions of WF beams such that these members may develop large plastic deformations without local buckling and a consequent fall-off in load. These later requirements are essential for a successful application of Plastic Design Methods.

7. ACKNOWLEDGEMENTS

This investigation has been carried out as part of the project "Welded Continuous Frames and Their Components" being conducted under the general direction of Dr. Lynn S. Beedle at the Fritz Engineering Laboratory, Lehigh University, Bethlehem, Pennsylvania. Professor W.J. Eney is director of Fritz Engineering Laboratory and head of the Civil Engineering Department.

The project is sponsored jointly by the Welding Research Council and the Department of the Navy with funds furnished by American Institute of Steel Construction, American Iron and Steel Institute, Column Research Council (Advisory), Office of Naval Research (Contract 39303), Bureau of Ships and Bureau of Yards and Docks.

The helpful criticisms of the Welding Research Council, Lehigh Project Subcommittee (Mr. T.R. Higgins, Chairman) and the Column Research Council Research Committee C (Dr. G. Winter, Chairman) are sincerely appreciated. The assistance of numerous Fritz Laboratory staff members throughout the investigation is gratefully acknowledged.

8. REFERENCES

1. Timoshenko, S., "Theory of Elastic Stability" McGraw-Hill, New York 1936

2. Bleich, F., "Buckling Strength of Metal Structures" McGraw-Hill, New York 1952

3. Haaijer, G., "Plate Buckling in the Strain-Hardening Range" Proceedings of the ASCE, Paper No.1212, April 1957

4. Nadai, A., "Theory of Flow and Fracture of Solids" McGraw-Hill, New York 1950

5. Huber, A.W., "The Influence of Residual Stress On The Instability of Columns" PhD Dissertation, Lehigh University, 1956

6. Huber, A.W., and Beedle, L.S., "Residual Stress and the Compressive Strength of Steel" Welding Journal 33(12), 1954

7. Kaufmann, W., "Bemerkungen zur Stabilität Dünnwandiger Kreiszylindrischer Schalen Oberhalb der Proportionalitäts Grenze" Ingenieur-Archiv, 1935, Vol. VI No.6.

8. Bijlaard, P.P., "Some Contributions to the Theory of Elastic and Plastic Stability", Pubs. Intern. Assoc. for Bridge & Structural Engineering, Vol. VIII, 1947

9. Ilyushin, A.A., "Stability of Plates and Shells Beyond the Proportional Limit", NACA TM-1116, October, 1947

10. Stowell, E.Z., "A Unified Theory of Plastic Buckling of Columns and Plates", NACA Report 898, 1948

11. Handelman, G.H., Prager, W., "Plastic Buckling of a Rectangular Plate with Edge Thrust", NACA. TN-1530, 1948

12. Haaijer, G., and Thürlimann, B., "Combined Compression and Torsion of Steel Tubes in the Strain-Hardening Range" Fritz Laboratory Report 241.2, Lehigh University (in preparation)

9. NOMENCLATURE

A = area

A_w = area of web

b = width of plate with one free edge

$D_x = \frac{E_x}{1 - \nu_x \nu_y}$

$D_y = \frac{E_y}{1 - \nu_x \nu_y}$

$D_{xy} = \nu_y D_x$

$D_{yx} = \nu_x D_y$

d = width of plate supported along all four edges

E = modulus of elasticity

E_o = strain-hardening modulus

E_r = reduced modulus

E_{sec} = secant modulus

E_t = tangent modulus

E_x = tangent modulus in x-direction

E_y = tangent modulus in y-direction

G = modulus of elasticity in shear

G_t = tangent modulus in shear

I = moment of inertia

K = coefficient in Equation (18)

k = plate buckling coefficient

L = length of column and WF compression specimen

L^* = length of WF specimen subjected to pure bending

ℓ = effective length of column

ℓ = half-wave length of buckled shape

M = bending moment

M_x = bending moment per unit width of plate in x-direction

M_y = bending moment per unit width of plate in y-direction

m = exponent in Equation (18)

n = exponent in Equation (26)

n_{max} = maximum value of n defined by Equation (27)

P = axial load

P_o = $\sigma_o A$ = yield load

r = radius of gyration

t = plate thickness

x = coordinate

y = coordinate

y_o = distance between neutral axis and compression flange

w = plate deflection

α = dimensionless coefficient defined by Eq.(24) and Eq.(25)

α_o = value of α at point of strain-hardening

β = coefficient of restraint

γ = shearing strain

ε = normal strain

ε_{av} = average strain

ε_{cr} = critical strain

ε_f = yield strain

ε_m = maximum strain of compression flange

ε_o = strain at beginning of strain-hardening

ζ = coefficient determining extent of yielding

θ = angle of lateral rotation

ν = Poisson's ratio

ν_x = coefficient of dilatation for stress increment in x-direction

ν_y = coefficient of dilatation for stress increment in y-direction

σ = normal stress

σ_{cr} = critical (buckling) stress

σ_e = elastic buckling stress

σ_p = stress corresponding to limit of validity of elastic solution

σ_o = yield stress

σ_R = residual stress

σ_r = reduced-modulus stress

σ_t = tangent-modulus stress

τ = shear stress

τ = E_t/E

ψ = edge moment per unit length to produce unit rotation of edge

TABLE 1

Comparison of Moduli as Predicted by Different Theories

Theory	E_x	E_y	G_t	ν_x	ν_y
Bleich (2)	E_t	E	$\frac{\sqrt{E \cdot E_t}}{2(1+\nu)}$	$\nu\sqrt{\frac{E_t}{E}}$	$\nu\sqrt{\frac{E}{E_t}}$
Kaufmann (7)	E_t	E	$\frac{E\,E_t}{(1+\nu)\,(E+E_t)}$	ν	ν
Bijlaard (8) Ilyushin (9) Stowell (10)	E_t	$\frac{E_t}{\frac{1}{4}+\frac{3}{4}\frac{E_t}{E_{sec}}}$	$\frac{E_{sec}}{3}$	$\frac{1}{2}$	$\frac{1}{\frac{1}{2}+\frac{3}{2}\frac{E_t}{E_{sec}}}$
Handelman and Prager (11)	E_t	$\frac{4EE_t}{E+3\,E_t}$	$\frac{E}{2(1+\nu)}$	$\frac{E_t(2\nu-1)+E}{2E}$	$\frac{2\left[E_t(2\nu-1)+E\right]}{E+3\,E_t}$

E = modulus of elasticity

ν = Poisson's ratio

E_t = tangent modulus = $\frac{d\sigma}{d\varepsilon}$

E_{sec} = secant modulus = $\frac{\sigma}{\varepsilon}$

TABLE 2

Dimensions of Short Columns

Specimen	b in.	t in.	L in.	$\ell/r = \frac{L}{2r}$
C2	0.745	0.544	2.80	8.9
C3	0.745	0.543	3.20	10.2
C4	0.745	0.543	3.65	11.6
C5	0.745	0.545	4.33	13.9
C6	0.745	0.545	4.80	15.3
C7	0.750	0.527	5.65	18.9
C8	0.750	0.527	6.90	23.4

b = width

t = thickness

L = length of specimen

$\ell/r = \frac{L}{2r}$ effective slenderness ratio (test conditions simulate fixed ends)

$r = \frac{t}{\sqrt{12}}$ = radius of gyration

TABLE 3

Dimensions of Angle Specimens

Specimen	Length 2ℓ (in)	Width b (in)	Thickness t (in)	b/t	2ℓ/b	Material
A-21	25.0	4.87	0.383	12.70	5.14	ASTM
A-22	25.0	4.79	0.381	12.60	5.21	A-7
A-31	17.9	3.27	0.370	8.85	5.48	Ann-
A-32	17.9	3.28	0.374	8.79	5.46	ealed
A-41	12.5	2.31	0.377	6.13	5.41	↓
A-42	12.5	2.34	0.371	6.36	5.35	
A-33	17.5	3.30	0.378	8.73	5.30	ASTM
A-51	21.2	4.07	0.380	10.70	5.21	A-7 As-delivered

TABLE 4

Results of Angle Coupon Tests

Coupon	Material	Yield Stress σ_o ksi	Strain at Strain-hardening $\varepsilon_o x 10^3$	Strain-hardening Modulus E_o ksi	Type of Loading
C1	Annealed	37.6	14.3	906	compression
C2	Annealed	35.1	14.6	845	"
T1	Annealed	36.8	18.5	903	tension
T2	Annealed	38.2	20.0	869	"
T3	As-delivered	40.2	9.5	877	"
T4	As-delivered	39.9	15.6	1,160	"

All coupons tested in Baldwin 60,000 lb. Hydraulic Machine. Valve opening corresponding to testing speed of 1 micro-in/in per second in the elastic range.

TABLE 5

Results of Angle Tests

Test	σ_o ksi	$\varepsilon_{cr} \cdot 10^3$	σ_{cr} ksi	Type of Buckling
A-22	--	3.0	32.2	torsional
A-31	34.9	16.5	35.8	torsional
A-32	34.6	16.5	35.6	torsional
A-41	35.3	--	--	bending
A-42	34.1	--	--	bending
A-33	41.3	16.0	46.4	torsional
A-51	41.0	6.0	41.2	torsional

TABLE 6

Dimensions of WF Specimens

Specimen	Shape	A in^2	Z in^3	2b in	t_f in	d in	t_w in	L in	L* in	b/t_f	d/t_w
B1 , D1	10WF33	9.66	38.56	7.95	0.429	9.37	0.294	32	32	9.2	31.9
B2 , D2	8WF24	6.83	22.56	6.55	0.383	7.63	0.236	26	26	8.6	32.3
B3 , D3	10WF39	11.34	45.63	8.02	0.512	9.37	0.328	32	32	7.8	28.6
B4 , D4	12WF50	14.25	70.28	8.18	0.620	11.57	0.351	32	32	6.6	33.0
B5 , D5	8WF35	10.00	33.68	8.08	0.476	7.65	0.308	32	32	8.5	24.8
B6 D6	10WF21	5.84	22.45	5.77	0.318	9.56	0.232	23	26	9.1	40.9

A = area of cross-section

Z = plastic section modulus (twice the static moment of half the section about the strong axis)

2b = width of flange

t_f = thickness of flange

d = distance between center planes of flanges

t_w = thickness of web

L = length of compression specimen

L^* = length of part of bending specimen subjected to pure bending

TABLE 7

Results of Coupon Tests

Coupon	Section	Buckling Tests	Location (see sketch)	Yield Stress σ_y ksi	Strain at Strain-hardening $\varepsilon_{st} \times 10^3$	Strain-hardening Modulus E_{st} ksi	Type of Loading
T6	10WF33	B1-D1	1	35.5	16.5	675	tension
T7			5	35.0	14.7	750	tension
C14			2	40.0	14.5	855	compression
C15			6	37.0	13.8	805	compression
T21	8WF24	B2-D2	1	35.4	18.4	530	tension
T22			2	35.6	18.0	600	tension
T23			3	36.3	19.3	470	tension
T31	10WF39	B3-D3	1	35.6	14.3	525	tension
T32			2	36.8	18.9	580	tension
T33			3	37.8	16.3	580	tension
T41	12WF50	B4-D4	1	37.1	18.0	500	tension
T42			2	36.9	18.1	530	tension
T43			3	39.4	15.9	580	tension
T51	8WF35	B5-D5	1	37.6	16.9	560	tension
T52			2	37.3	16.6	465	tension
T53			3	39.9	19.6	600	tension
T61	10WF21	B6-D6	1	38.0	20.8	520	tension
T62			2	34.2	23.4	570	tension
T63			3	44.2	23.6	490	tension

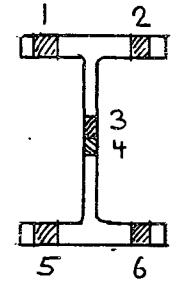

Location of Coupons

All coupons tested in Baldwin 60,000 lb. Hydraulic Machine.

Valve opening corresponding to testing speed of 1 micro-in/in per sec. in the elastic range.

TABLE 8

Results of WF Tests

Test	σ_o ksi	$\varepsilon_{cr} \cdot 10^3$		σ_{cr} ksi		Flange ℓ/b	Web ℓ/d	Type of Buckling
		Flange	Web	Flange	Web			
D1	34.4	8.5	8.5	34.2	34.2	1.8	0.56	flange
D2	34.0	13.5	12.7	34.0	34.0	1.5	0.50	flange & web
D3	35.2	19.0	19.0	39.0	39.0	1.5	0.46	flange
D4	35.0	18.5	5.0	36.8	35.4	1.5	0.55	web
D5	36.6	17.0	17.0	38.0	38.0	2.1	0.56	flange
D6	38.0	4.3	1.6	33.8	37.2	--	0.54	web
B1	-	7.0	-	-	-	2.4	-	flange
B2	-	23.0	-	-	-	2.0	-	flange & lateral
B3	-	22.5	-	-	-	2.2	-	flange & lateral
B4	-	29.0	-	-	-	-	-	lateral
B5	-	22.0	-	-	-	2.0	-	flange & lateral
B6	-	14.0	-	-	-	2.4	-	flange & lateral

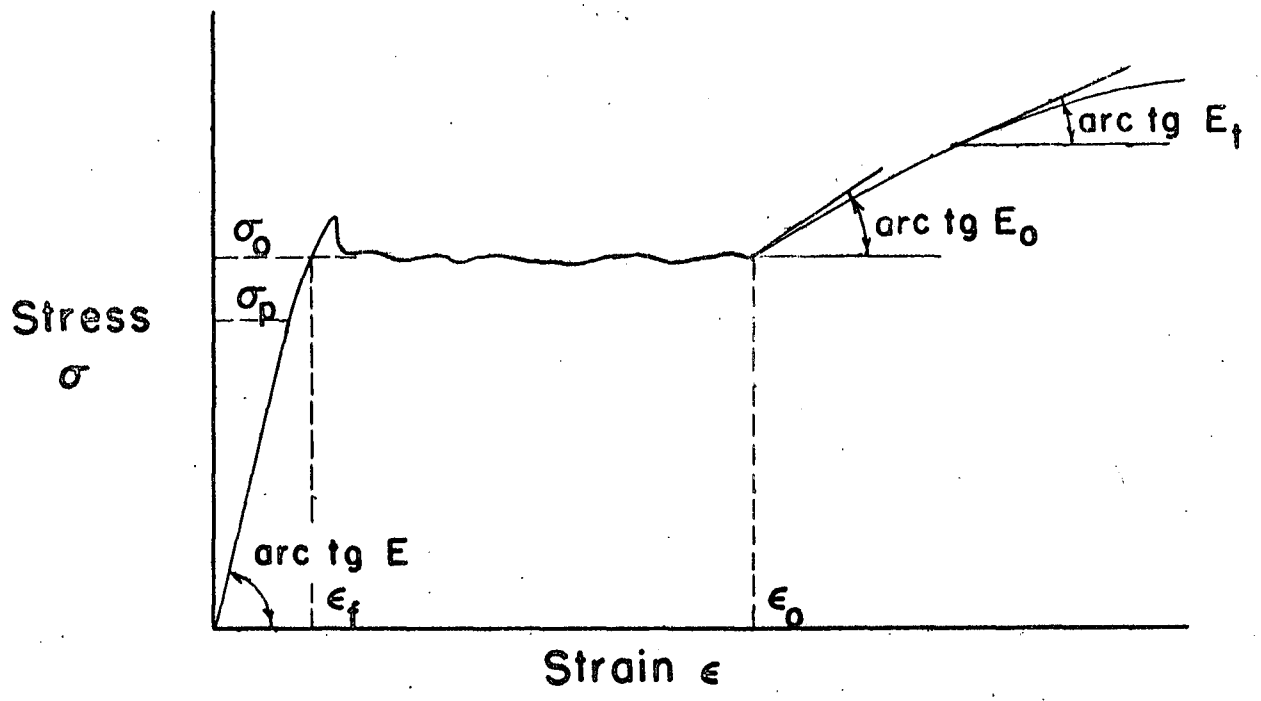

Fig. 1a. Typical Stress-Strain Curve of Mild Steel

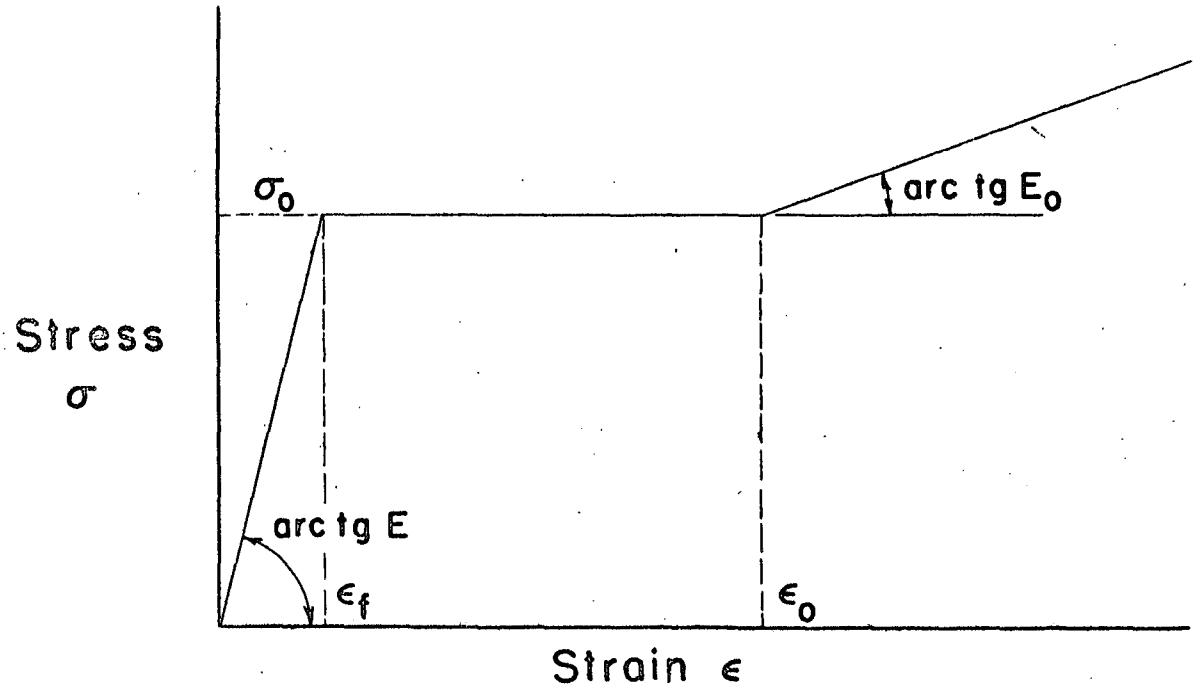

Fig. 1b. Simplified Stress-Strain Curve

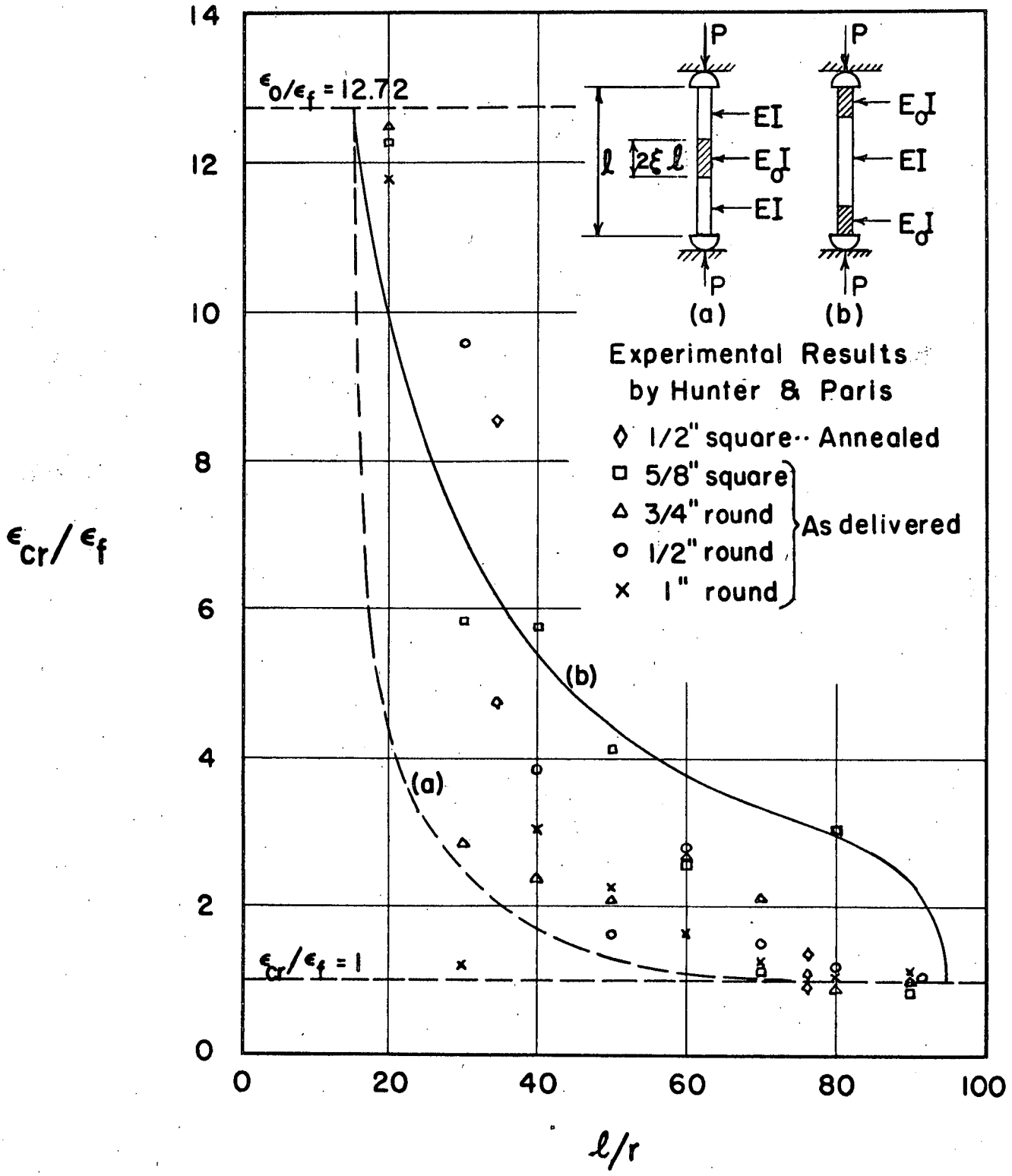

Fig. 2 Comparison of Theoretical Curves with Results of Model Column Tests

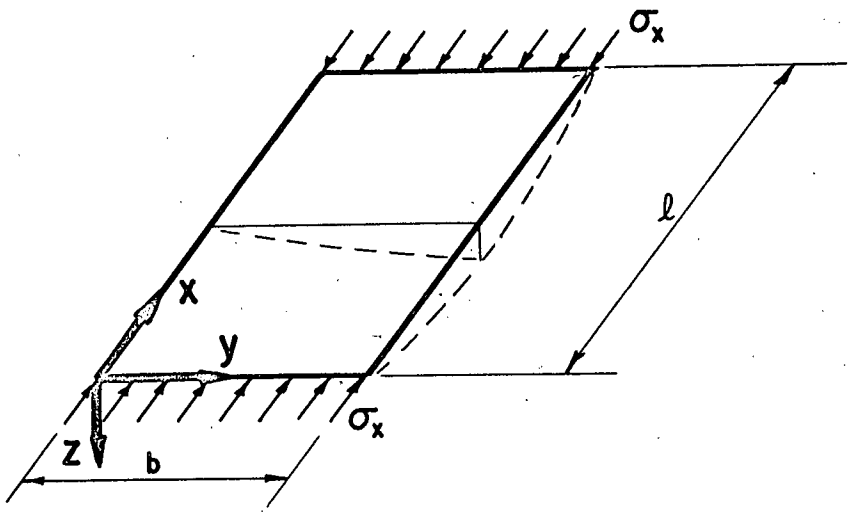

Fig. 3 Plate with one free edge

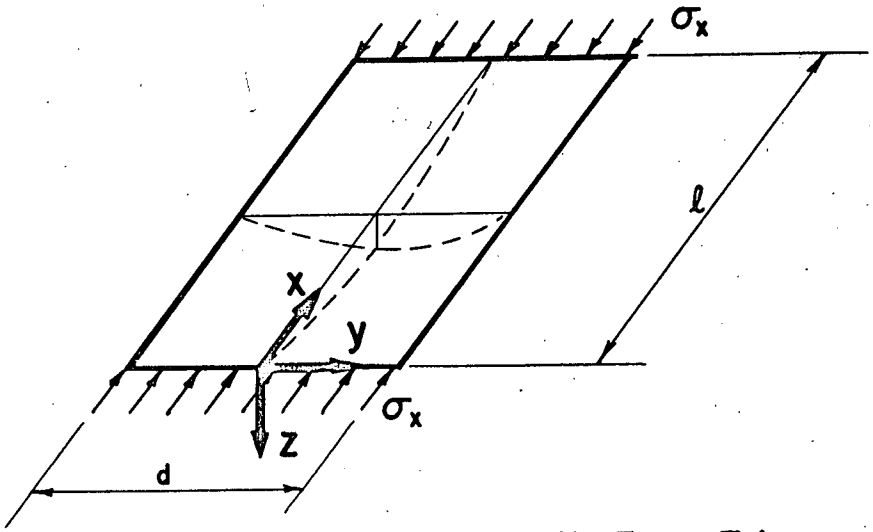

Fig. 4 Plate Supported Along All Four Edges

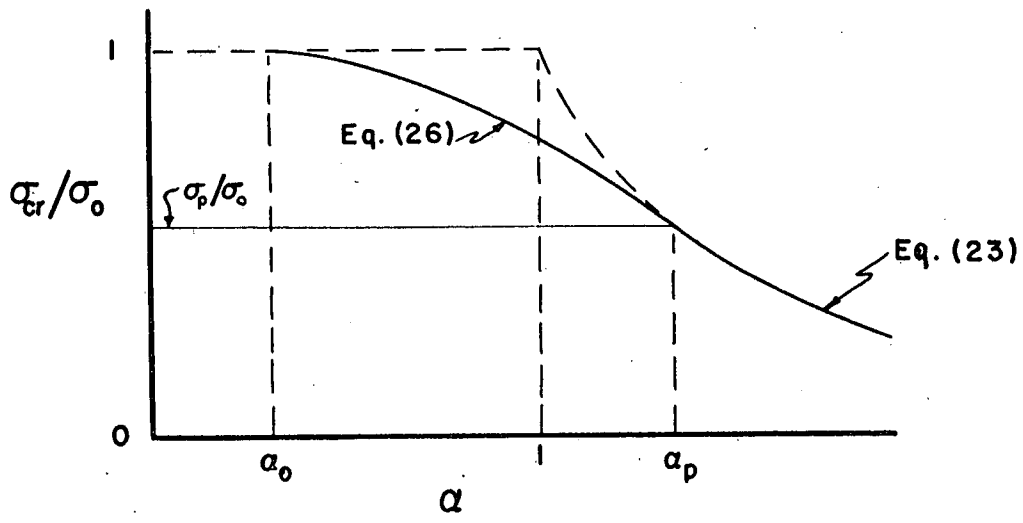

Fig. 5 Dimensionless Representation of the Buckling Strength of Columns and Plates

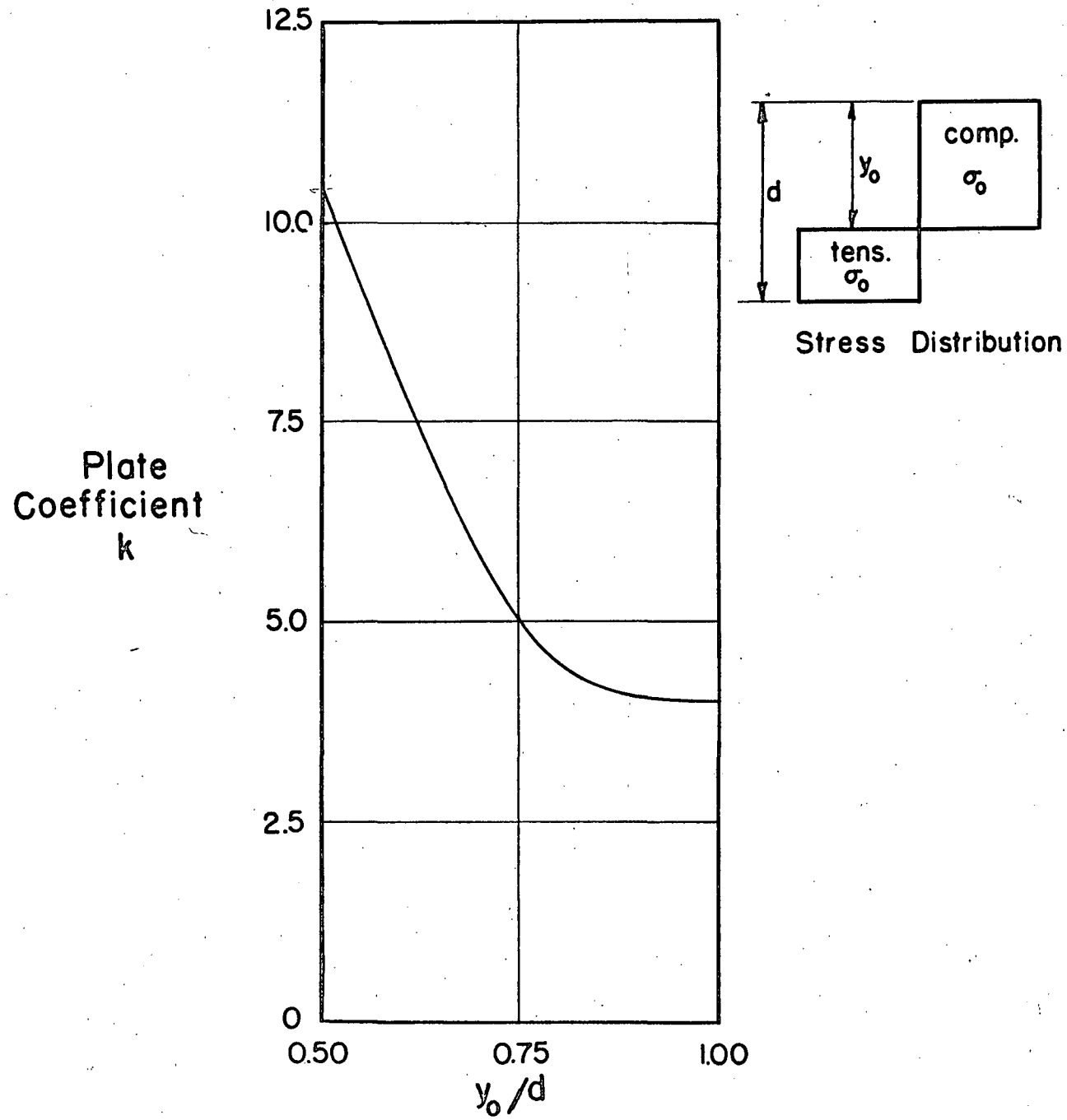

Fig. 6 Plate Coefficient of Webs of Fully Plastified Wide-Flange Sections Subjected to Axial Load and Moment.

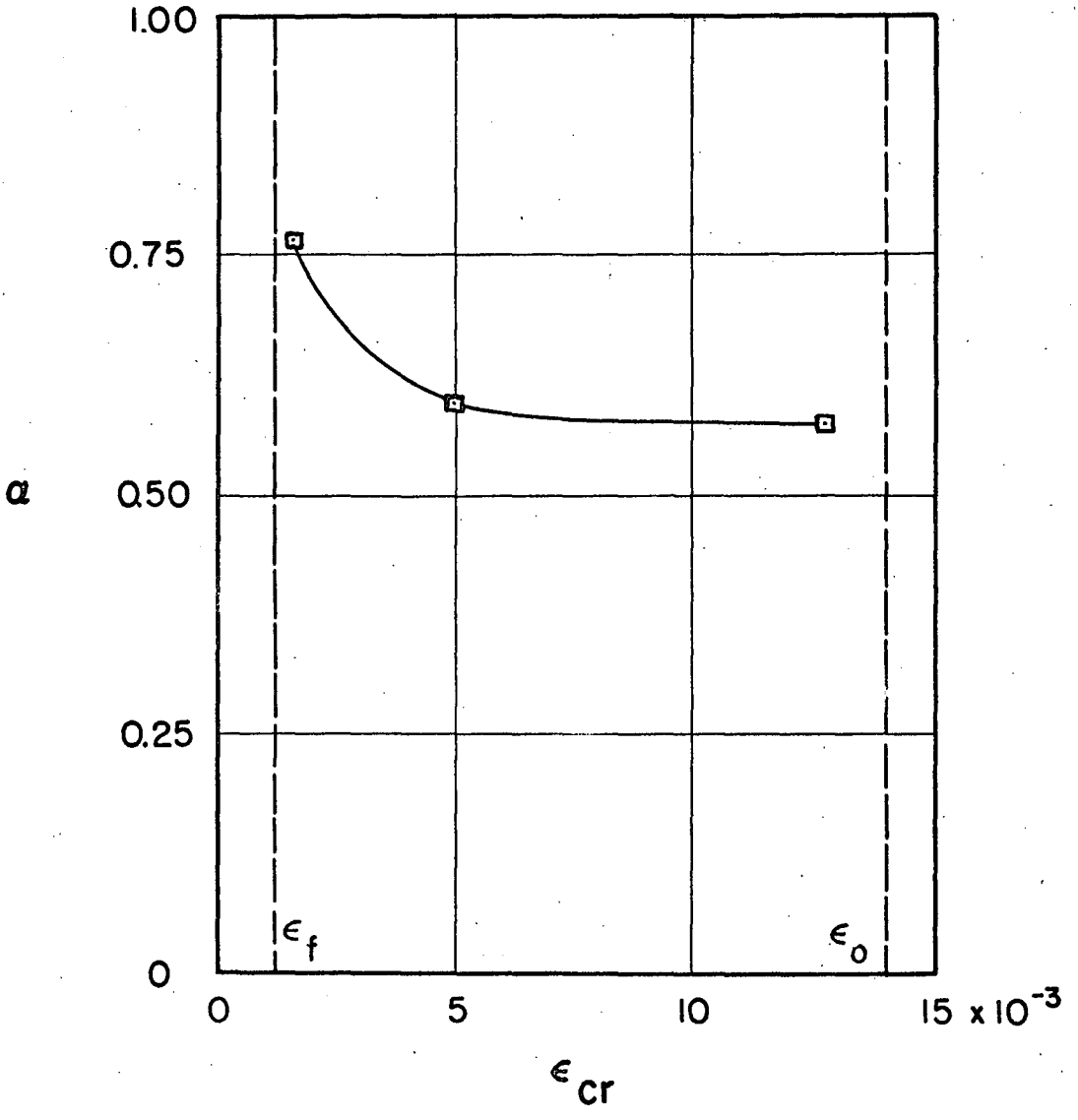

Fig. 7 Experimentally Determined Values of α as a Function of the Critical Strain of Uniformly Compressed Webs.

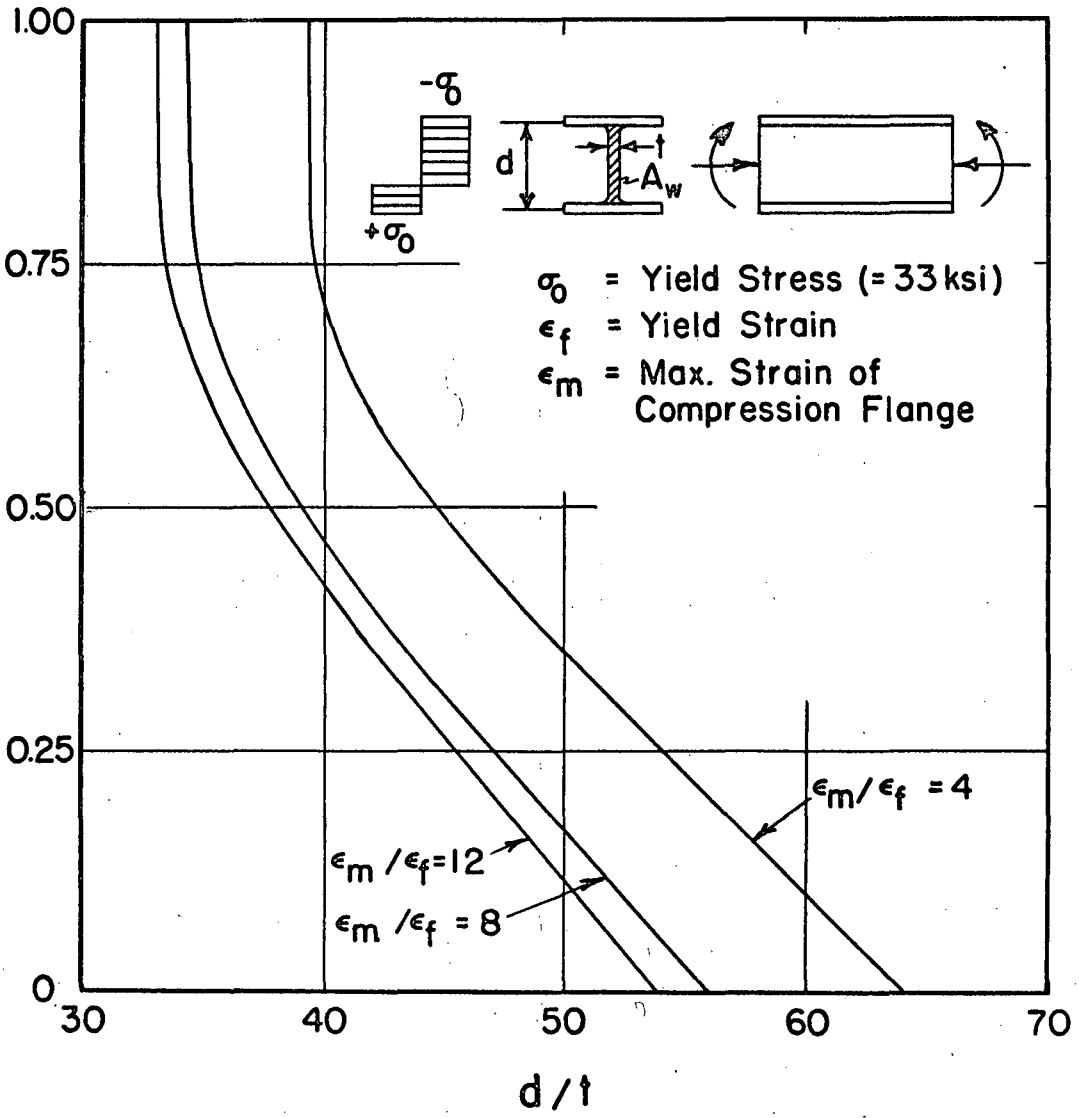

Fig. 8 Allowable d/t Ratios of Webs of Fully Plastified WF Sections for σ_0 = 33 ksi

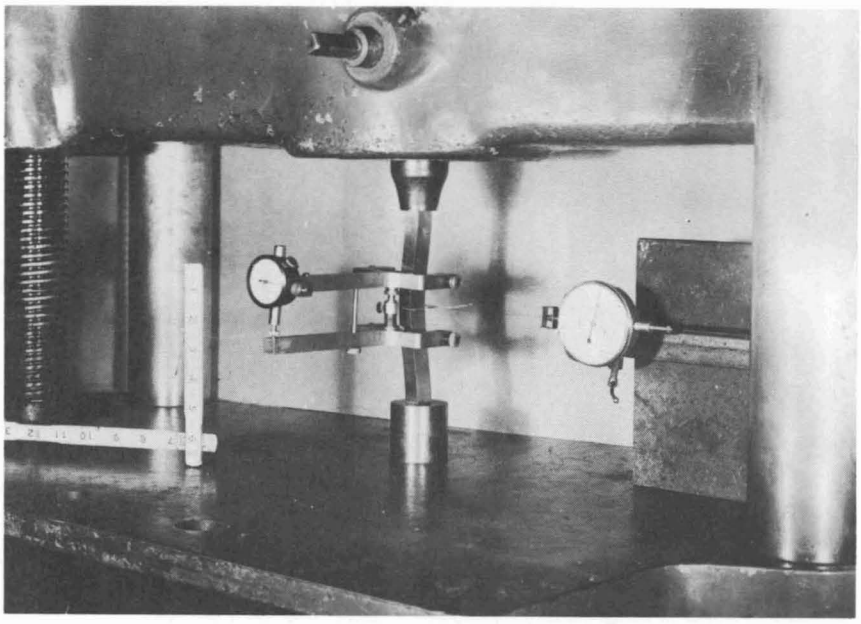

Fig. 9. Short Column Test

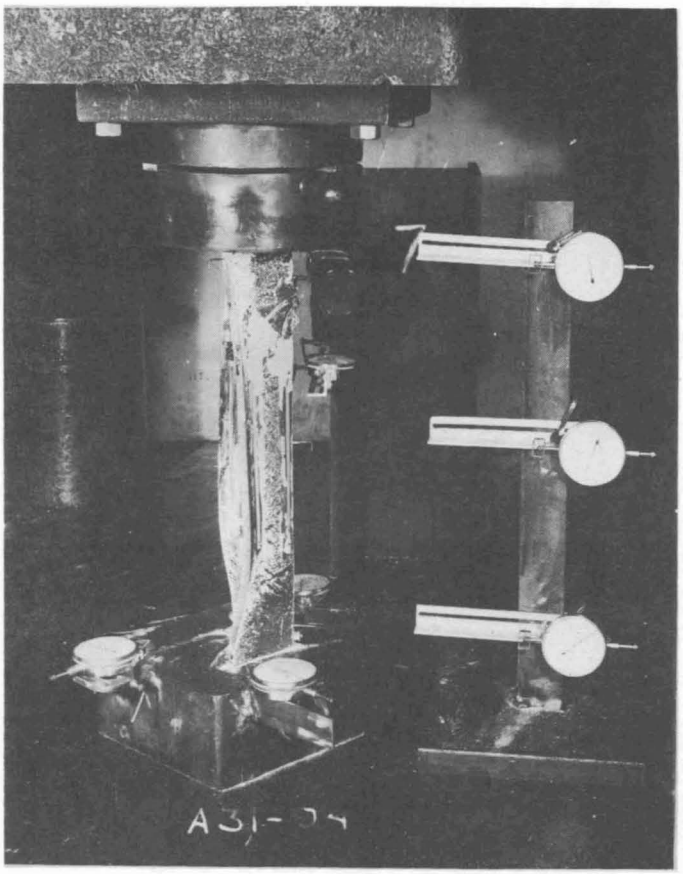

Fig. 10 Angle Test

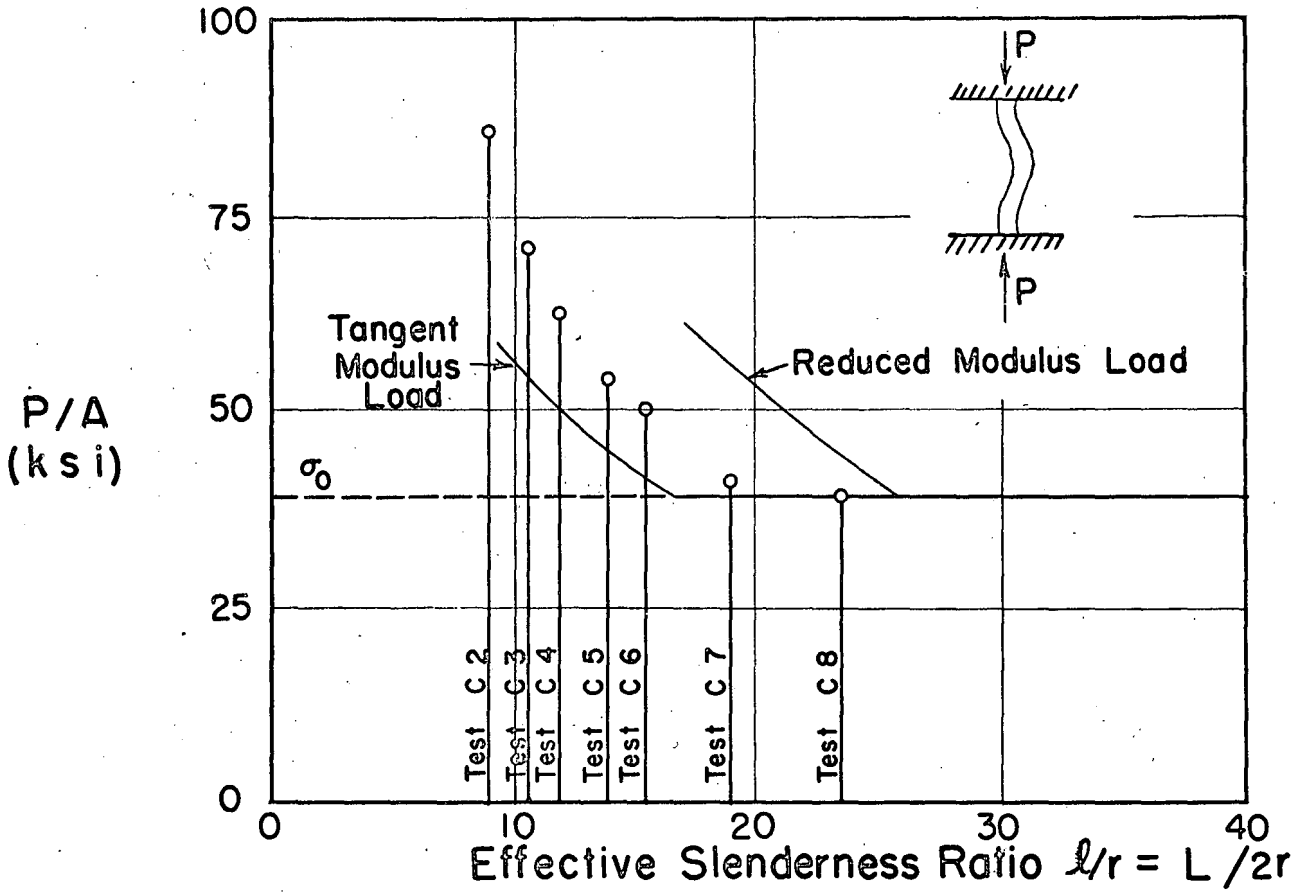

Fig. 11 Comparison of Maximum Loads of Short Columns with Tangent- and Reduced-Modulus Loads

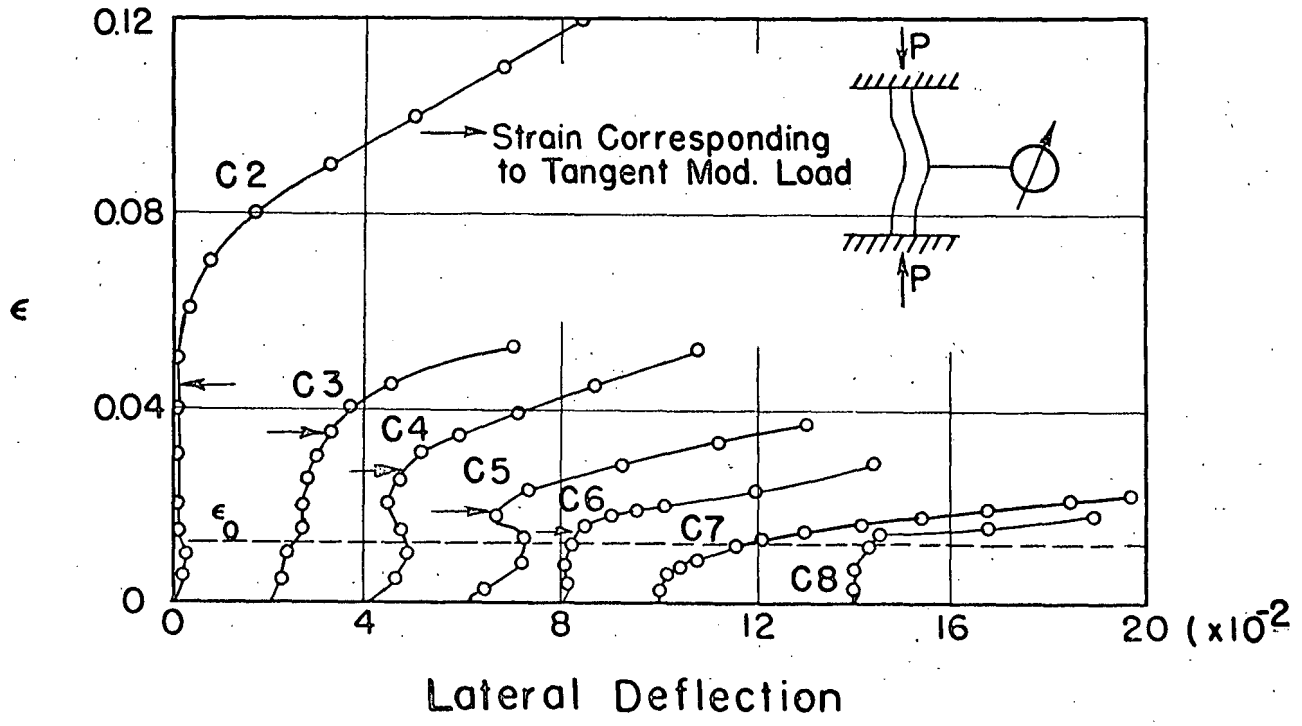

Fig. 12 Lateral Deflection of Short Columns

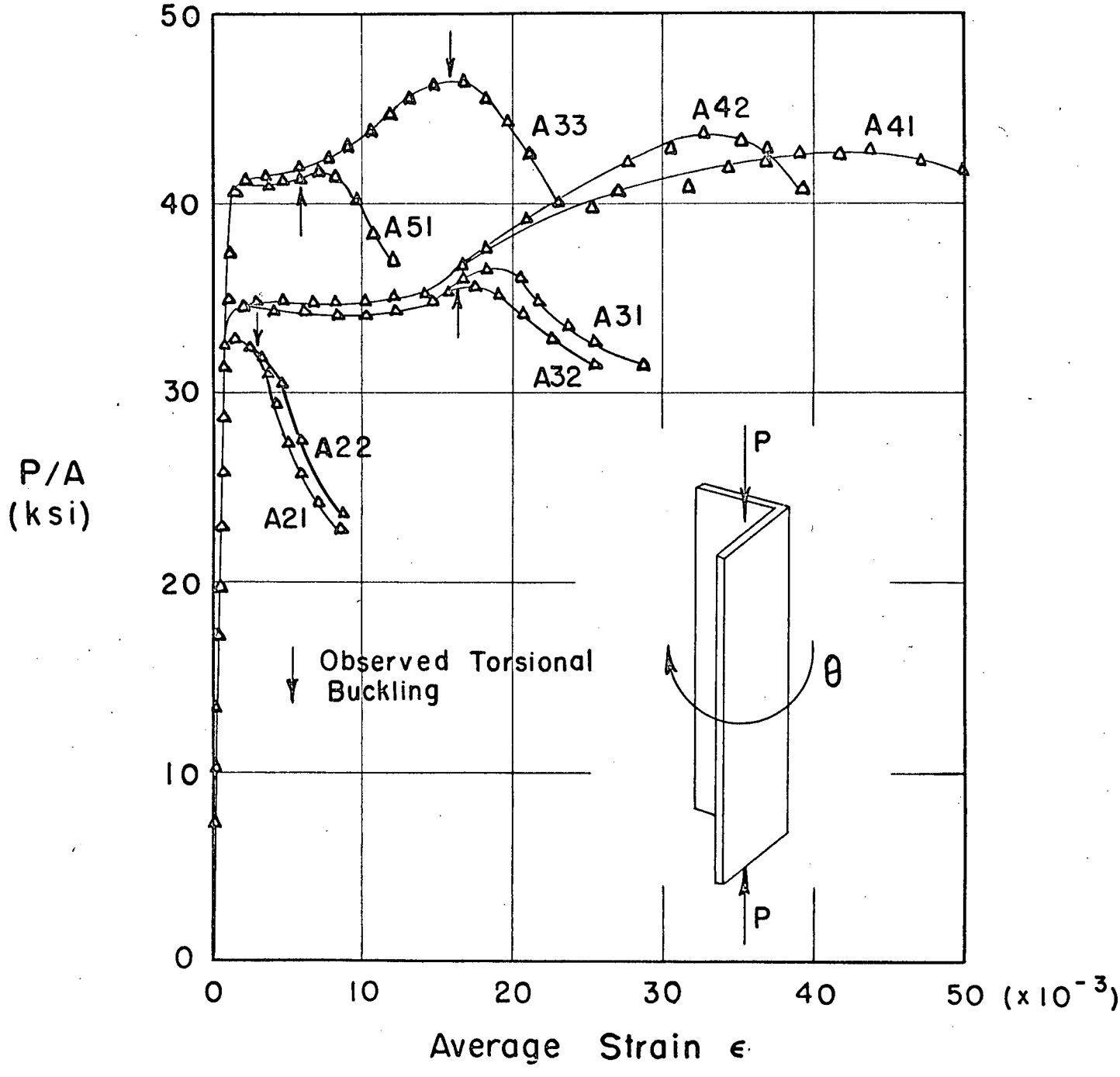

Fig. 13 Results of Angle Compression Tests

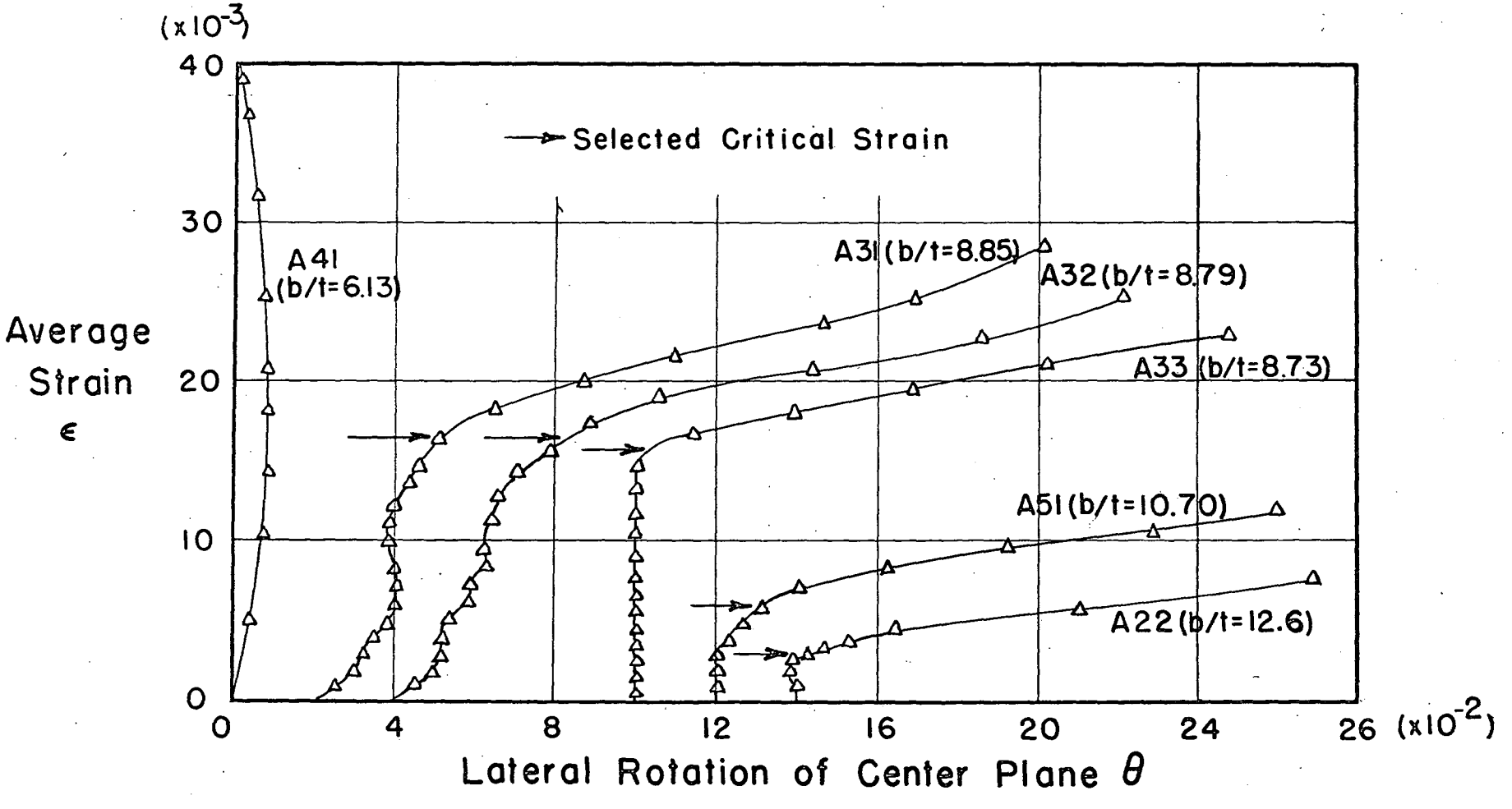

Fig. 14 Lateral Rotation of Angle Specimens

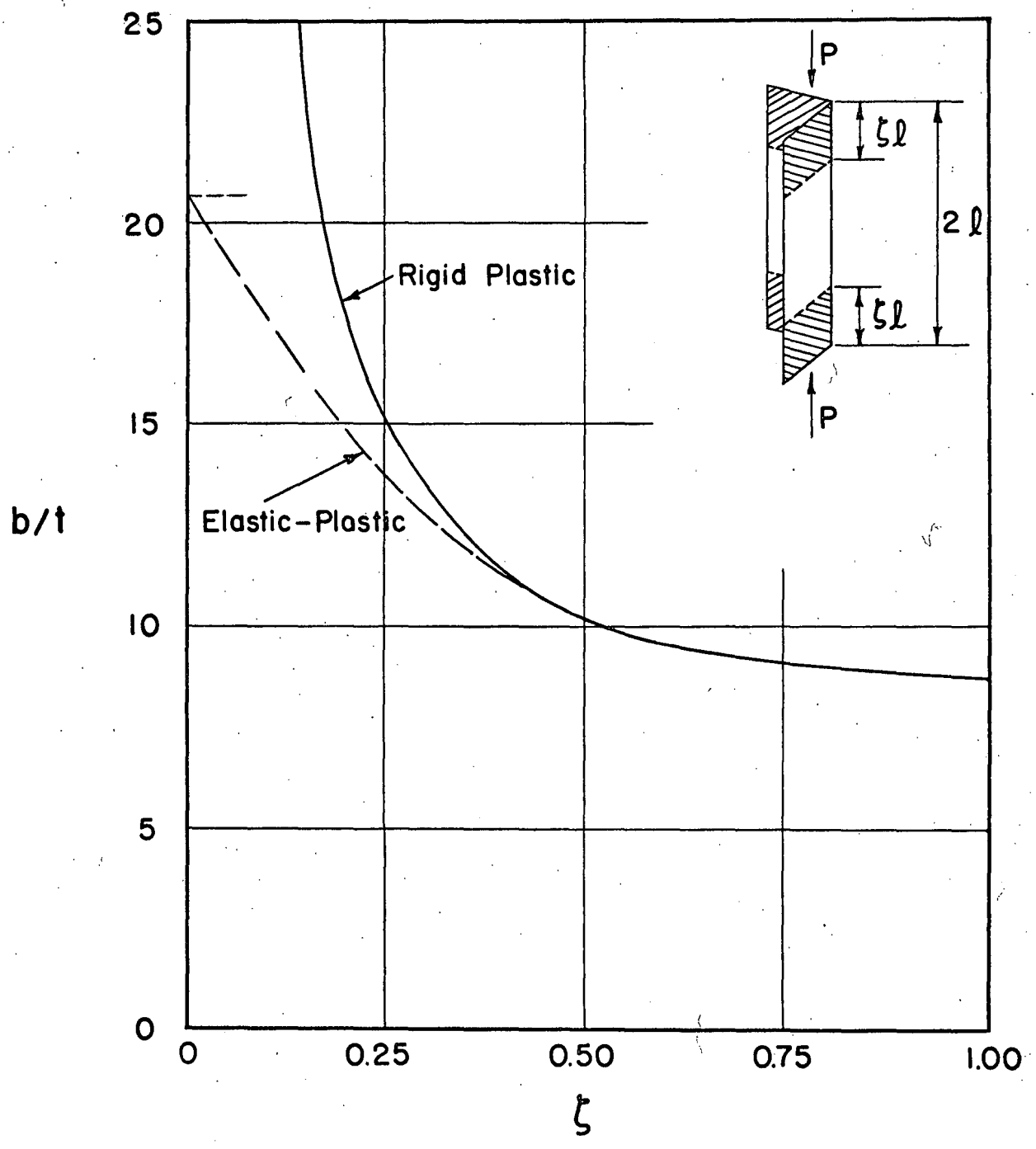

Fig. 15a Yield Penetration ζ as a Function of b/t for $\ell/b = 2.65$

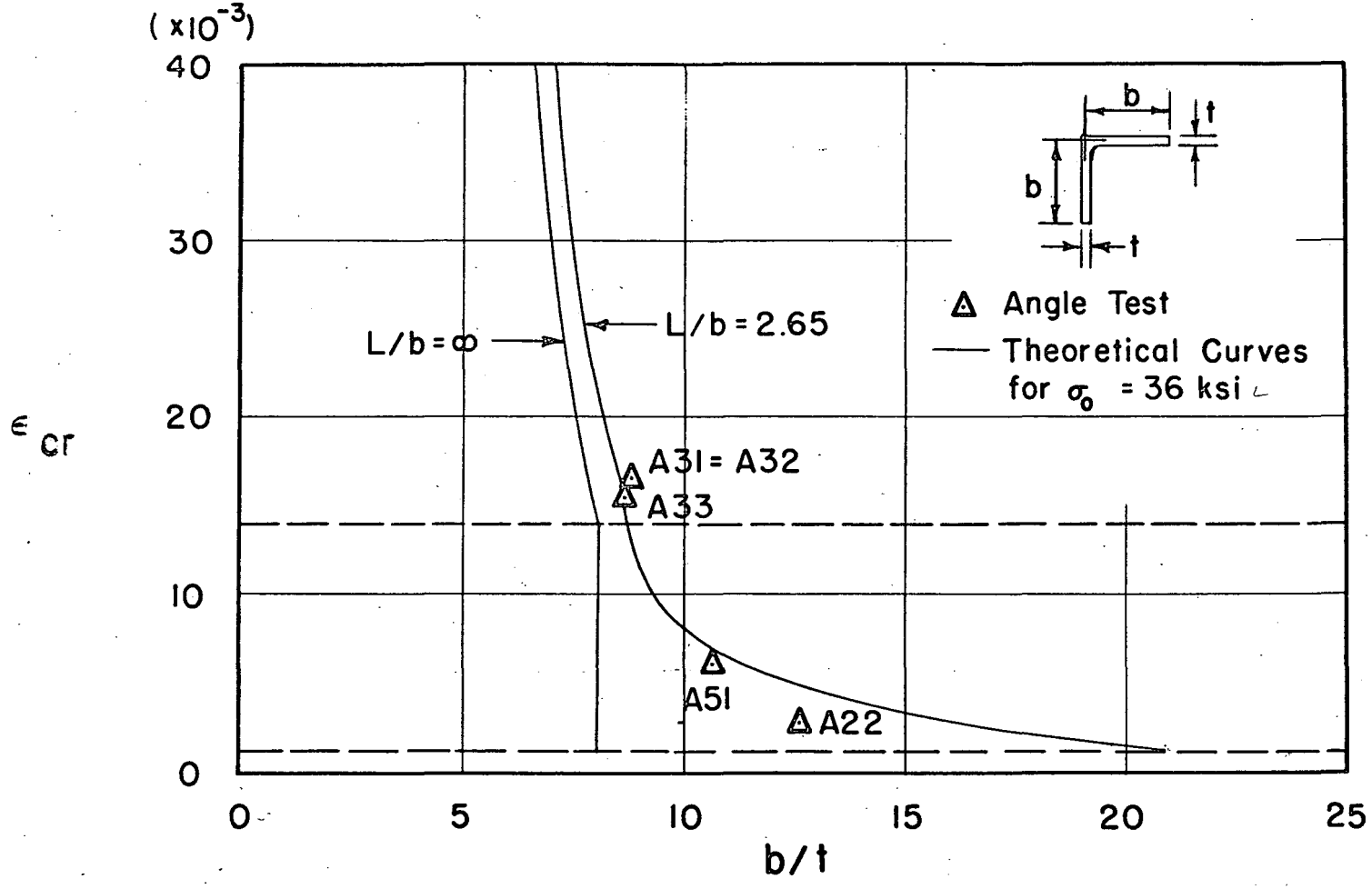

Fig. 15b Comparison of Results of Torsional Buckling Tests on Angles with Theoretical Curves

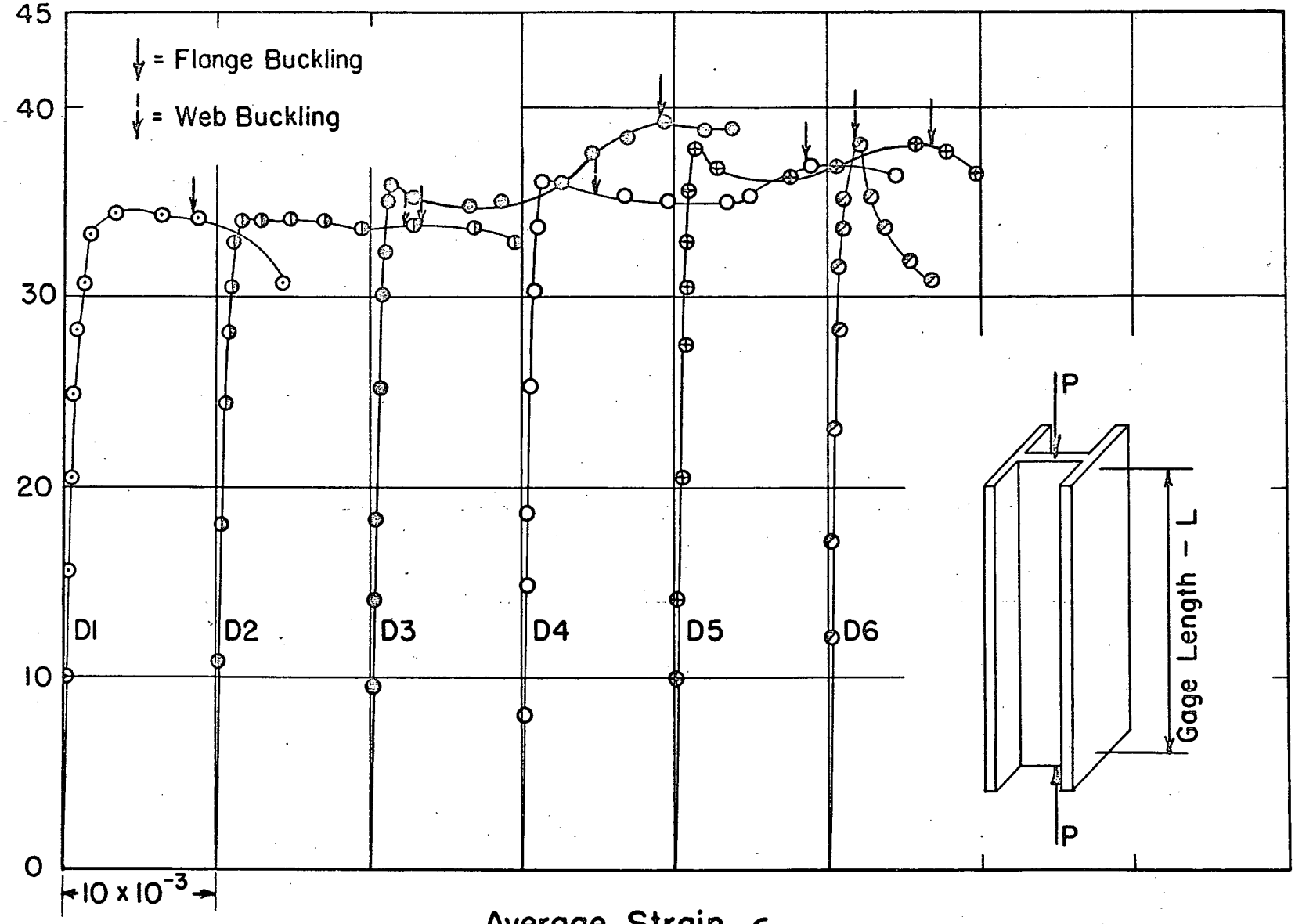

Fig. 16 Result of WF Compression Tests

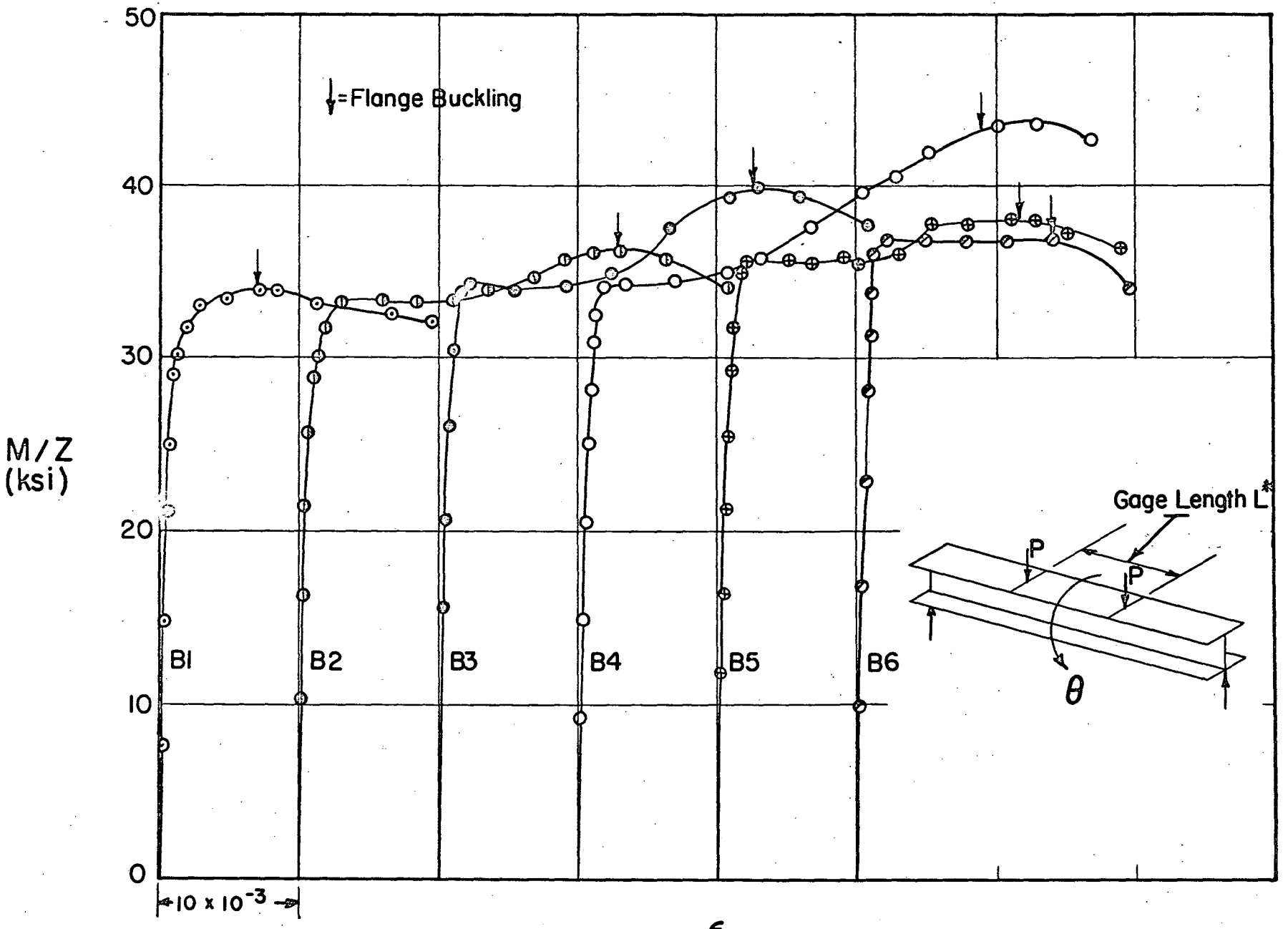

Fig. 17 Results of WF Bending Tests

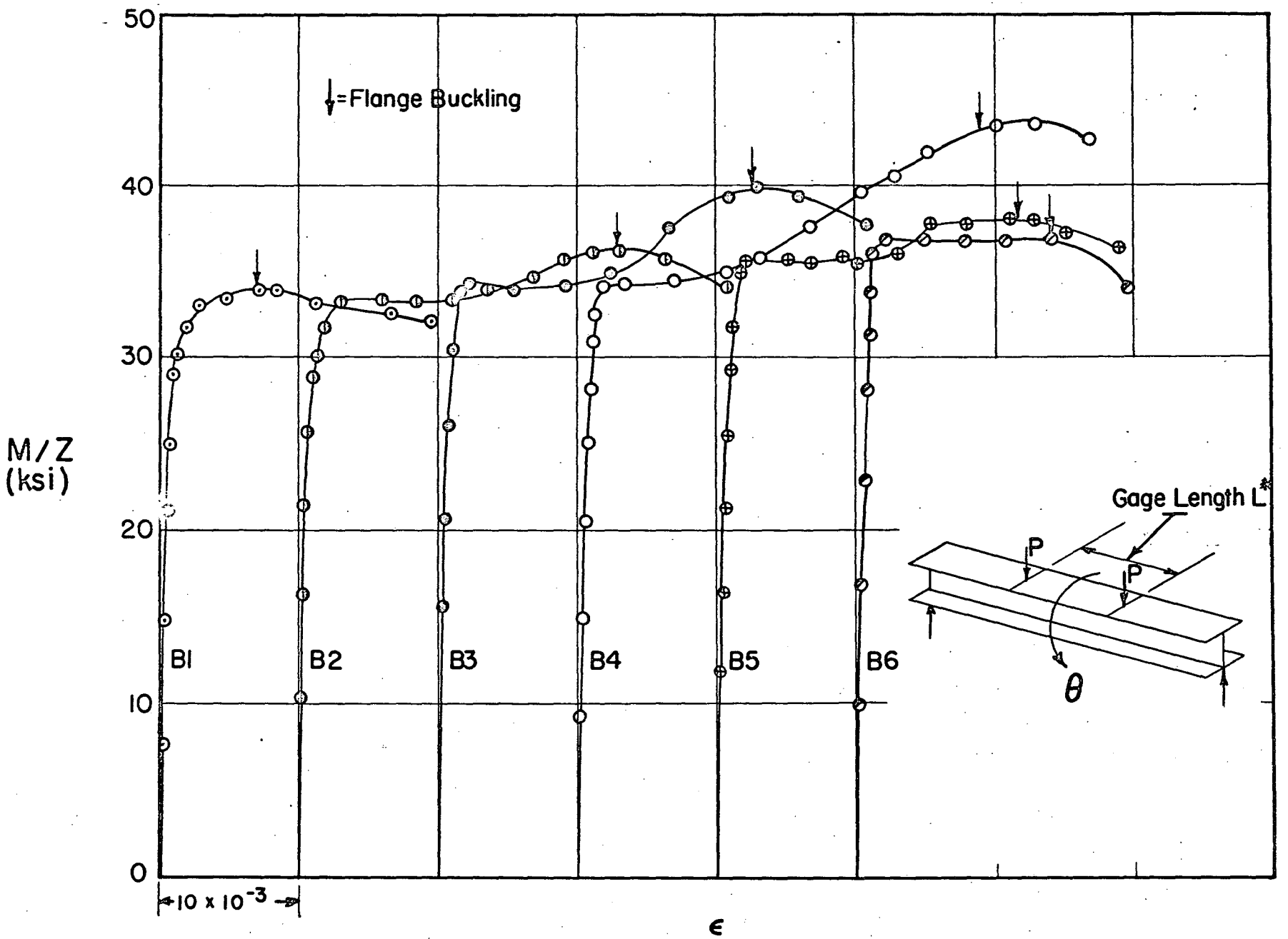

Fig. 17 Results of WF Bending Tests

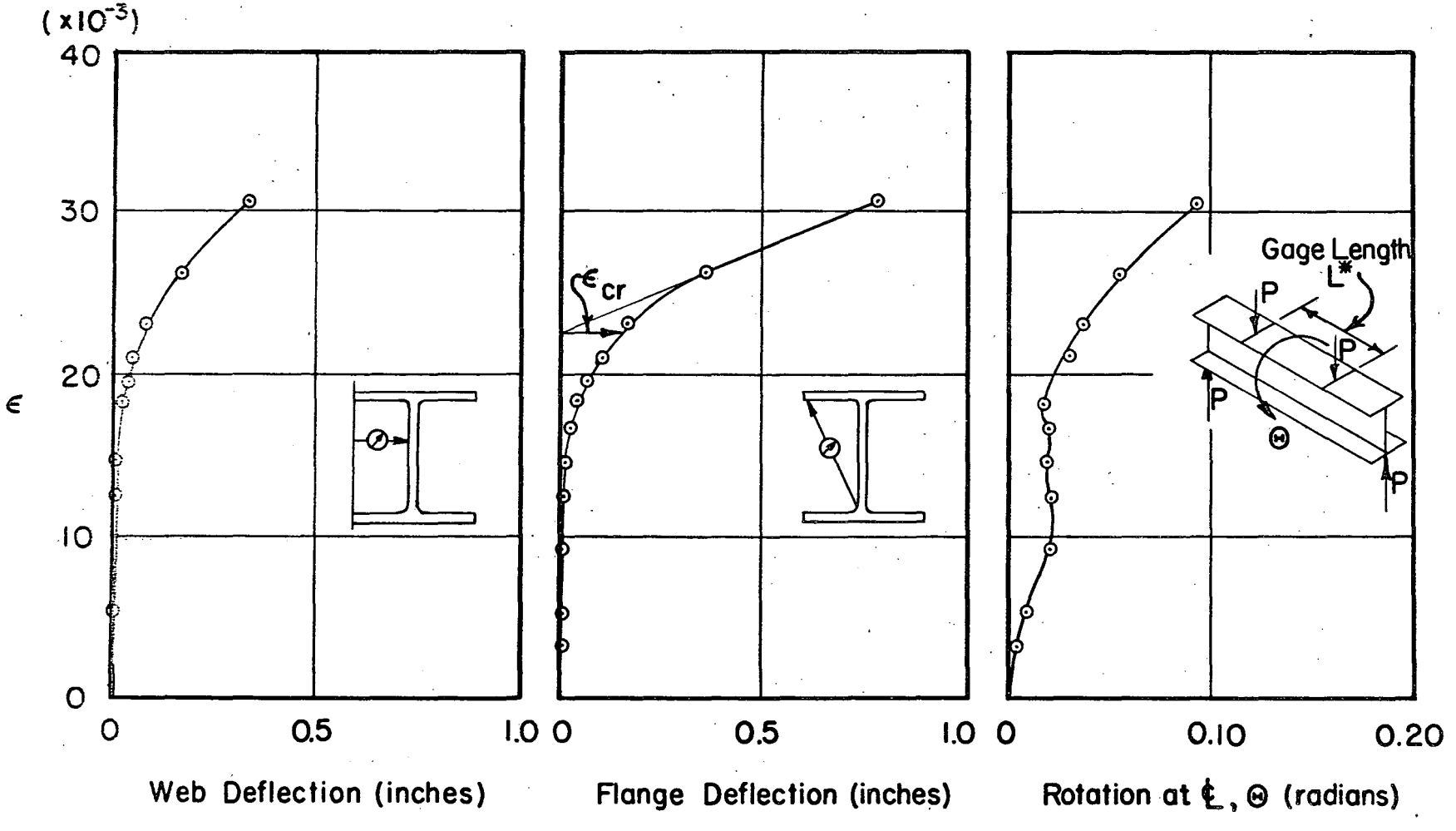

Fig. 18 Typical Curves for Lateral Web and Flange Deflections and Lateral Rotation (WF Bending Test B3)

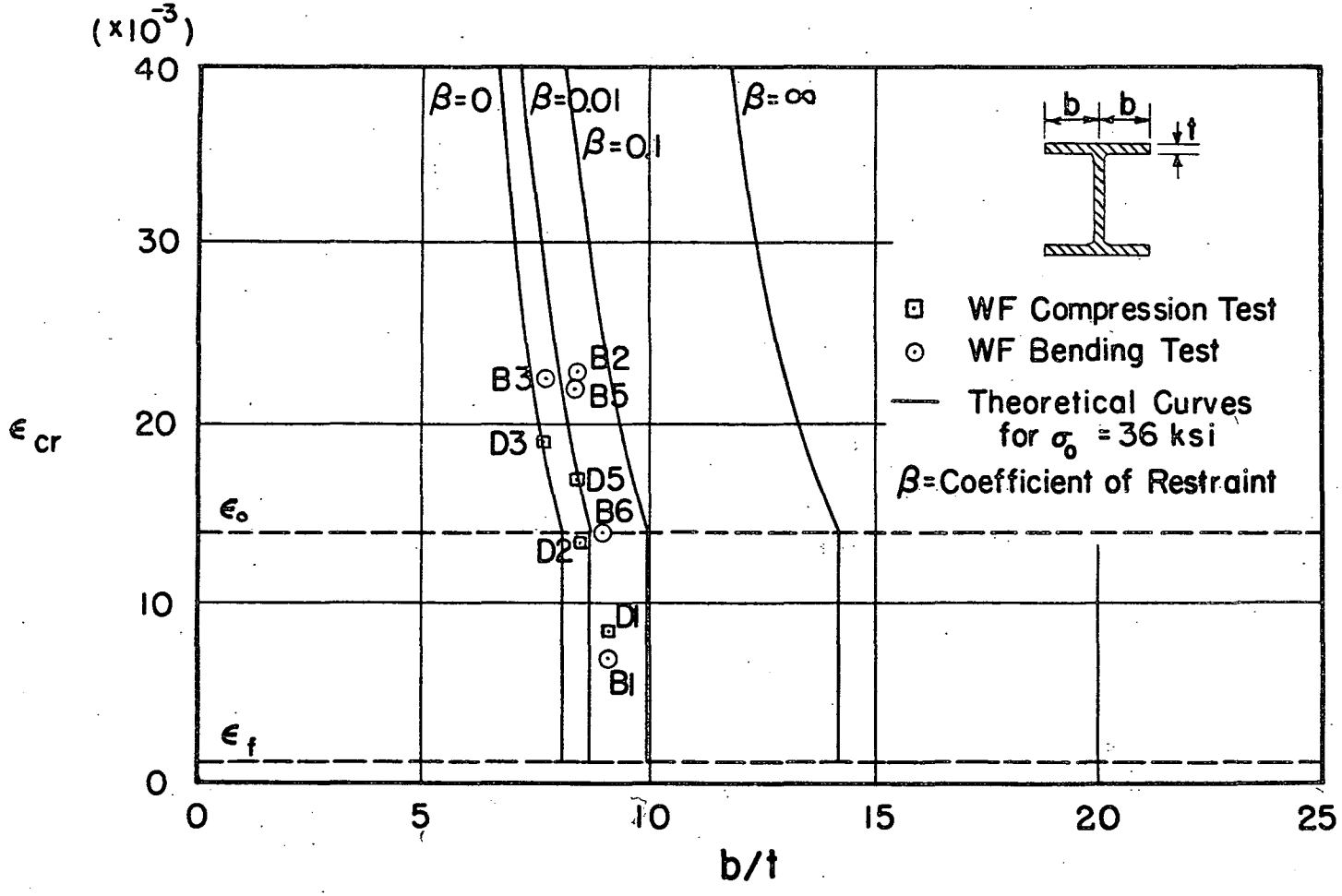

Fig. 19 Buckling of Flanges of Wide-Flange Shapes

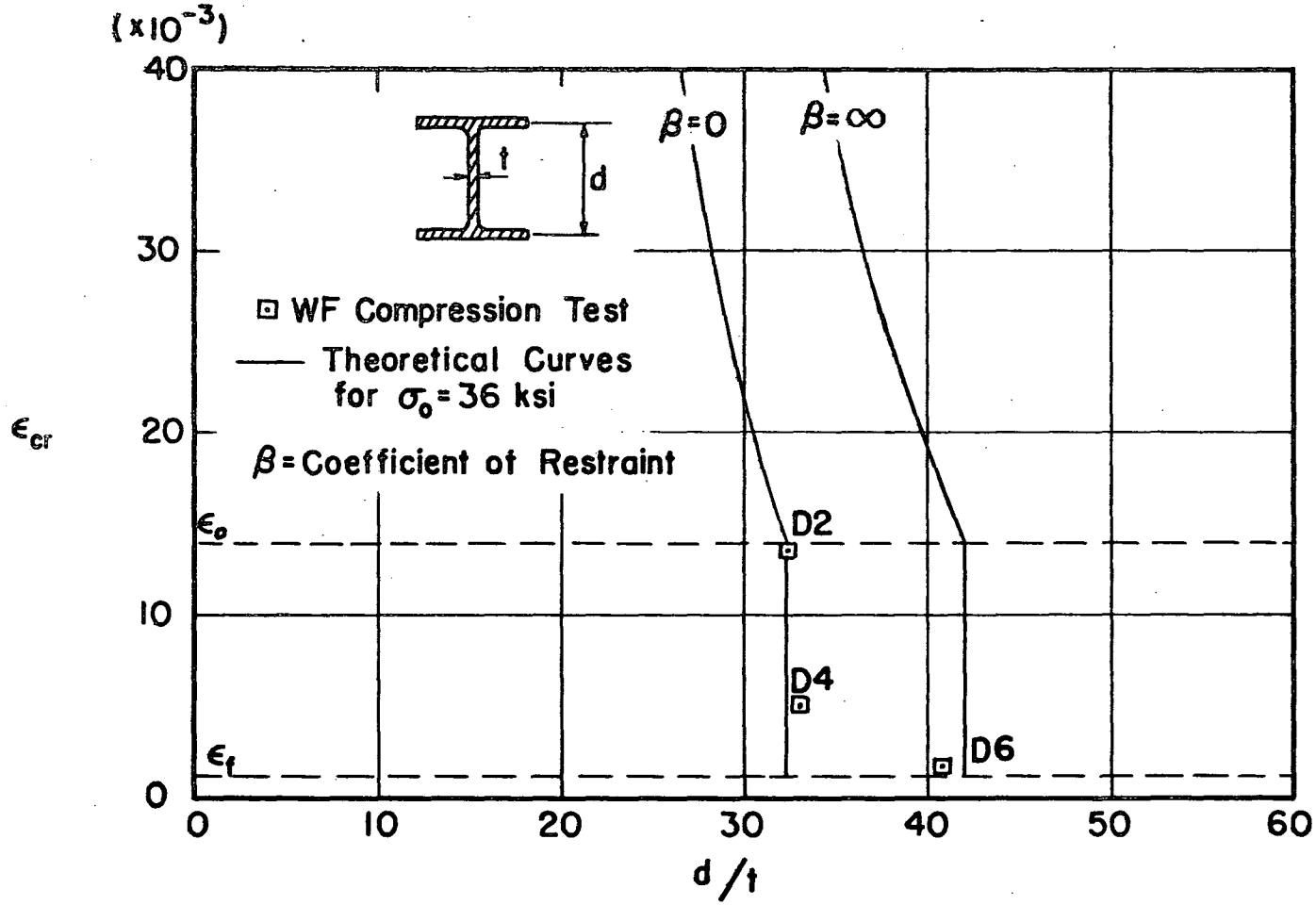

Fig. 20 Buckling of Webs of Wide-Flange Shapes (Uniform Compression)

Fig. 21a Wide-Flange Compression Test (D3)

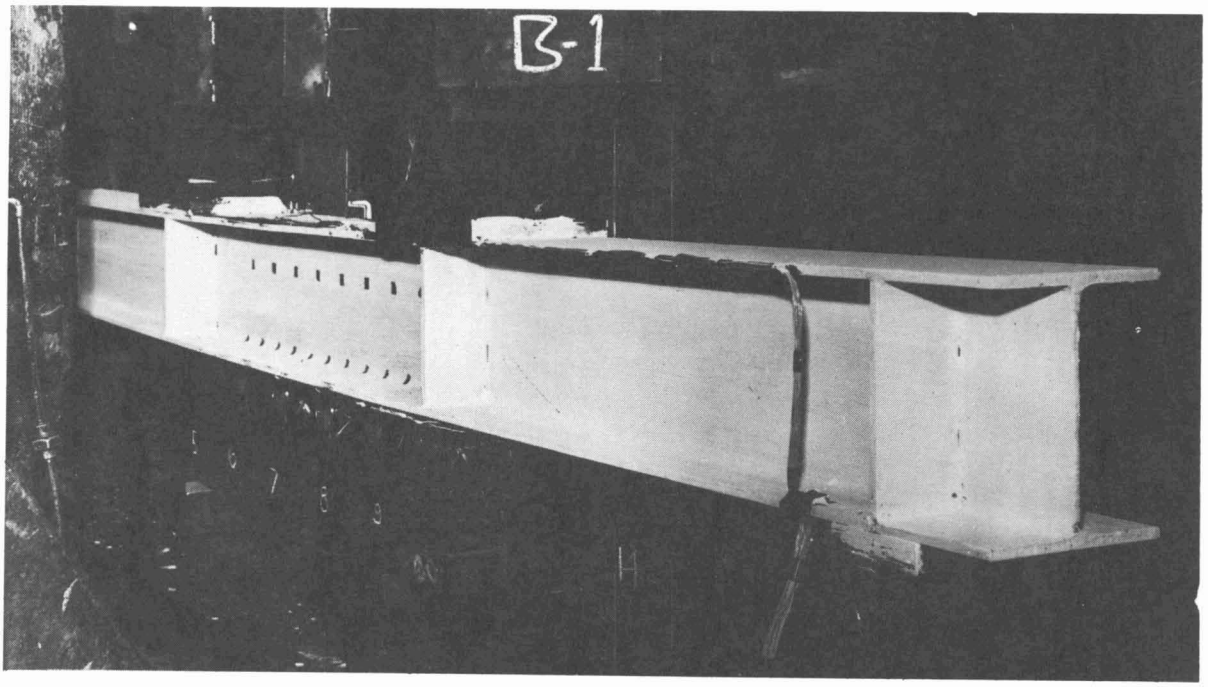

Fig. 21b Wide Flange Bending Test (B1)

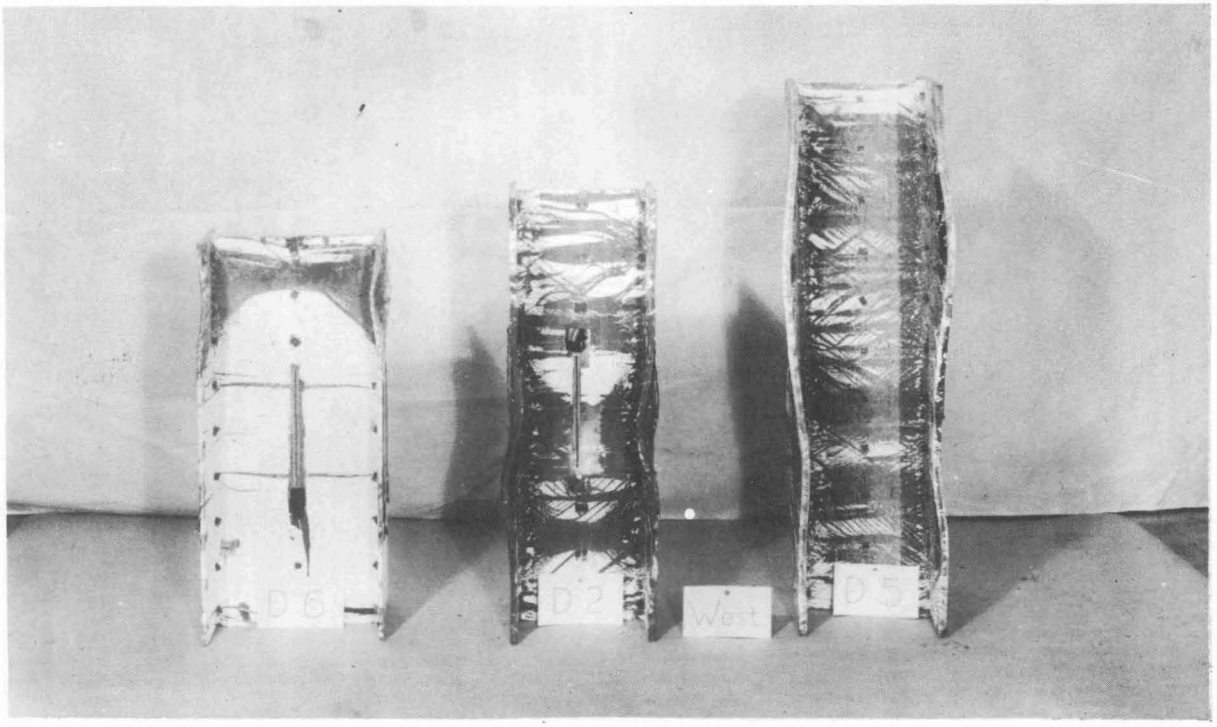

Specimen D6 Specimen D2 Specimen D5

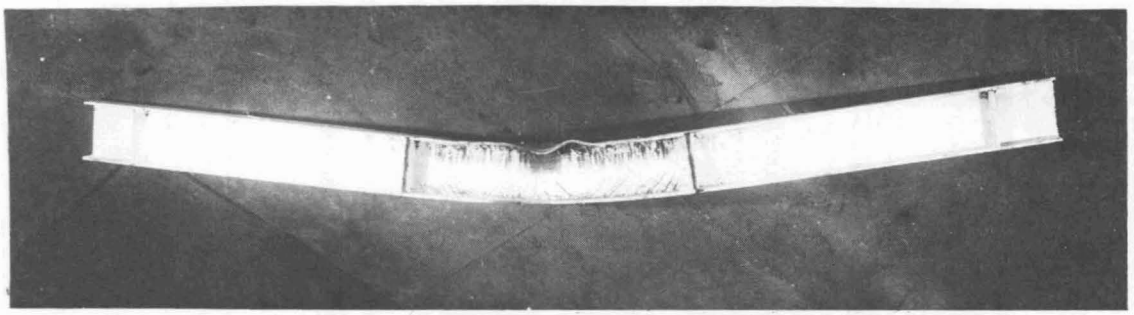

Specimen B2

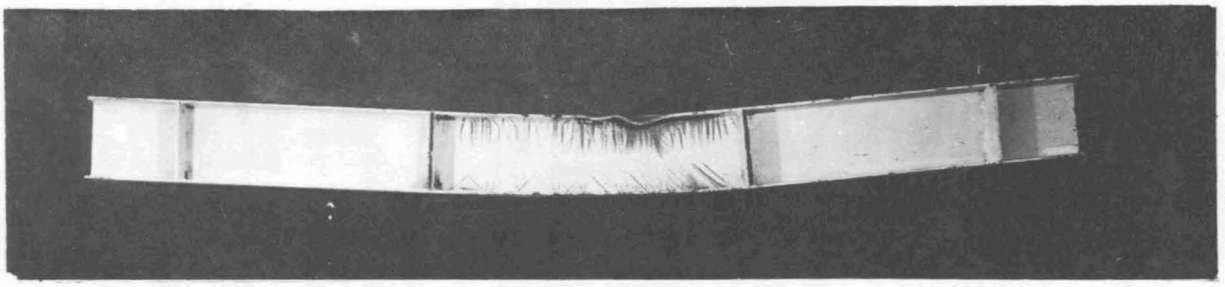

Specimen B6

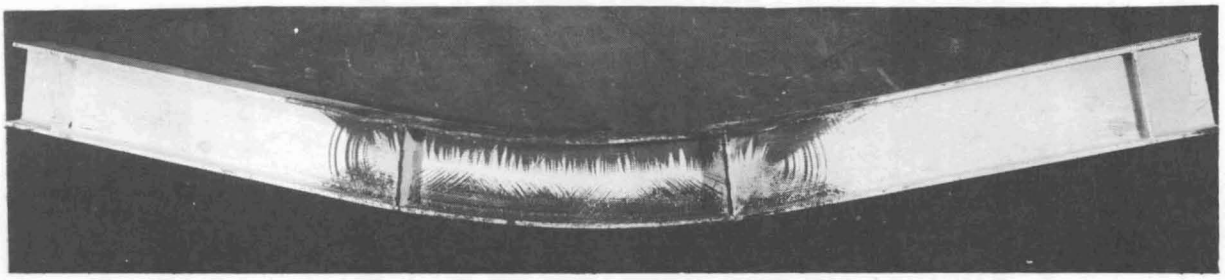

Specimen B4

Fig. 22 Typical Examples of Wide-Flange Specimens After Testing

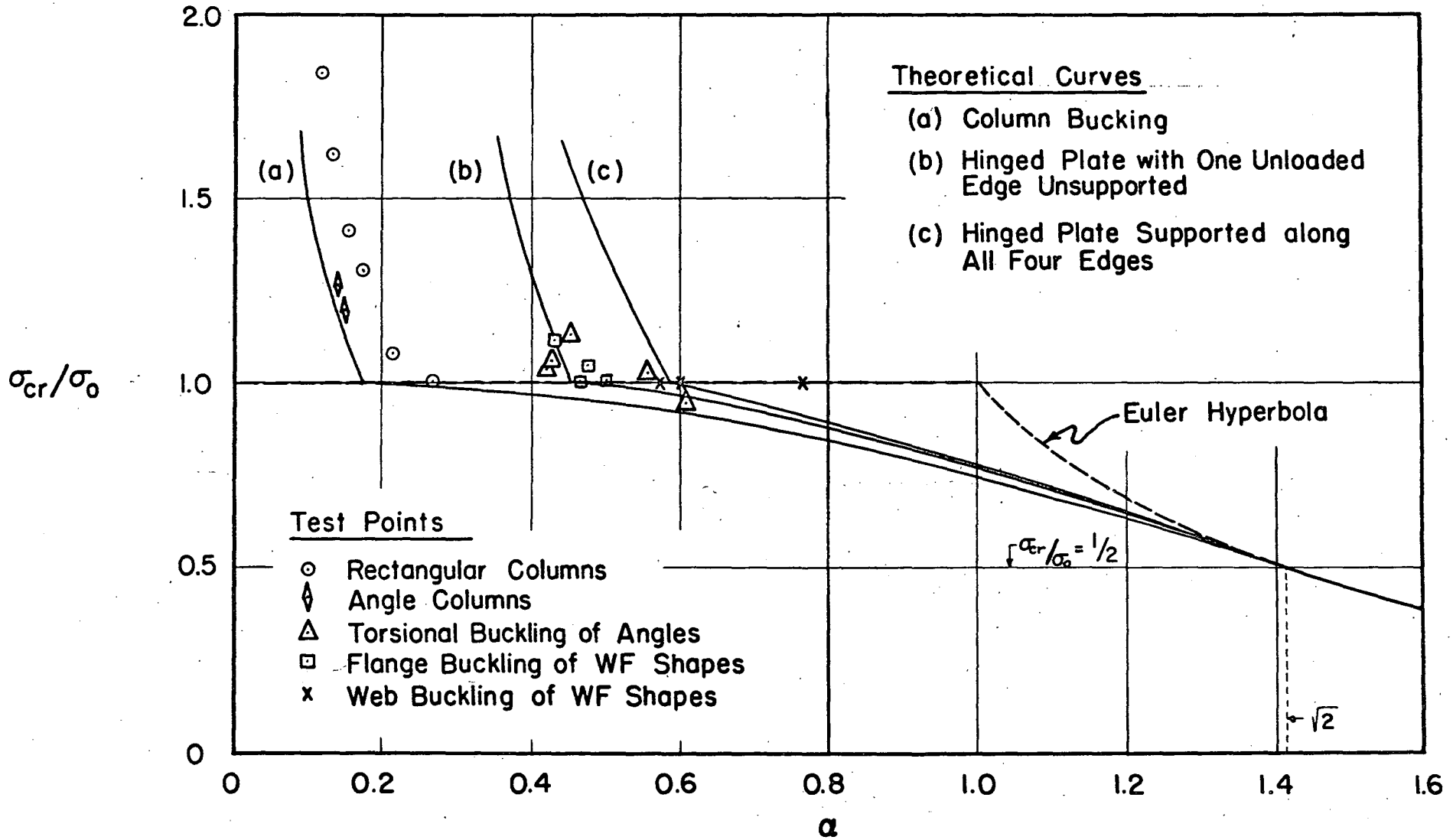

Fig. 23 Summary of Test Results and Theory

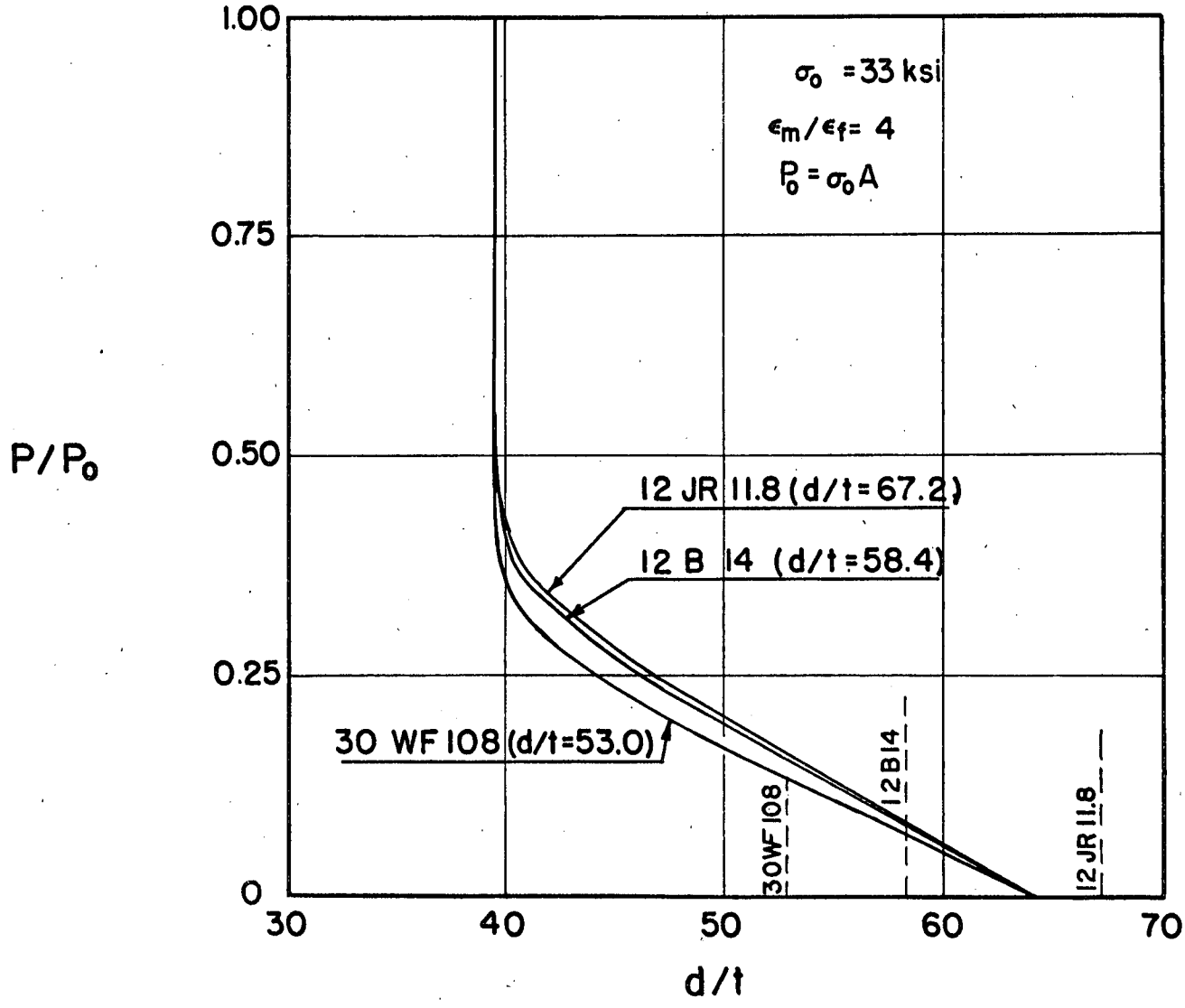

Fig. 24 Allowable d/t of Three Deep Section for $\epsilon_m/\epsilon_f = 4$ and $\sigma_0 = 33$ ksi